Partial Oxidation of Methane to Syngas Over Biomass Derived Catalyst

By

Amin ul Hasanat

Reg. No: 00000277540

Session 2018-2020

Supervisor

Dr Asif Hussain Khoja

U.S. –Pakistan Center for Advanced Studies in Energy (USPCAS-E)

National University of Sciences and Technology (NUST)

H-12, Islamabad 44000, Pakistan

January 2022

Partial Oxidation of Methane to Syngas Over Biomass Derived Catalyst

By

Amin ul Hasanat

00000277540

Session 2018-2020

Supervisor

Dr. Asif Hussain Khoja

A Thesis Submitted to U.S. – Pakistan Center for Advanced Studies in Energy in partial fulfillment of the requirements for the degree of

MASTERS of SCIENCE

in

THERMAL ENERGY ENGINEERING

U.S.– Pakistan Center for Advanced Studies in Energy (USPCAS-E)

National University of Sciences and Technology (NUST)

H-12, Islamabad 44000, Pakistan

January 2022

THESIS ACCEPTANCE CERTIFICATE

Certified that final copy of MS/MPhil thesis written by Mr. Amin ul Hasanat, (Registration No. 00000277540), of U.S.-Pakistan Center for Advanced Studies in Energy (USPCASE), NUST has been vetted by undersigned, found complete in all respects as per NUST Statues/Regulations, is in the allowable limits of plagiarism, errors, and mistakes and is accepted as partial fulfillment for award of MS/MPhil degree. It is further certified that necessary amendments as pointed out by GEC members of the scholar have also been incorporated in the said thesis.

Signature: _____

Name of Supervisor: Dr Asif Hussain Khoja

Date: _____

Signature (HoD TEE): _____

Date: _____

Signature (Principal/Dean): _____

Date: _____

Certificate

This is to certify that work in this thesis has been carried out by **Mr. Amin ul Hasanat** and completed under my supervision in Fossil Fuels laboratory, USPCAS-E, National University of Sciences and Technology, H-12, Islamabad, Pakistan.

Supervisor:

_____
Dr. Asif Hussain Khoja
U.S.-Pakistan Center for Advanced Studies in Energy
NUST, Islamabad

GEC member 1:

_____
Dr. Mustafa Anwar
U.S.-Pakistan Center for Advanced Studies in Energy
NUST, Islamabad

GEC member 2:

_____
Dr. Sehar Shakir
U.S.-Pakistan Center for Advanced Studies in Energy
NUST, Islamabad

GEC member 3:

_____
Dr. Salman Raza Naqvi
SCME
NUST, Islamabad

HoD-TEE:

_____
Dr. Majid Ali
U.S.-Pakistan Center for Advanced Studies in Energy
NUST, Islamabad

Principal:

_____
Prof. Dr. Adeel Waqas
U.S.-Pakistan Center for Advanced Studies in Energy
NUST, Islamabad

Acknowledgements

All praise and thanks to Allah Almighty, who provided me with the power and skills to comprehend, learn, and complete my thesis report.

It gives me great pleasure to express my heartfelt gratitude to my research supervisor, Dr. Asif Hussain Khoja, for allowing me to join the Fossil Fuels Lab study group, USPCAS-E, NUST, Islamabad. I consider myself fortunate to have worked under his supervision. It was a combination of his patience, perseverance, guidance, and inspiration that enabled me to complete my research goals on time. He showed me the approach for conducting research and presenting the findings as clearly as possible.

I owe a debt of gratitude to the members of my GEC committee, Dr. Mustafa Anwar, Dr. Sehar Shakir and Dr. Salman Raza Naqvi who honored my committee's presence. I'd want to express my gratitude to my colleagues and friends for their unwavering support. I'd want to express my gratitude to Lab Engineers Mr. Ali Abdullah for his unwavering assistance throughout the research.

I owe my parents, wife, and siblings a debt of gratitude for their love, prayers, care, and sacrifices.

Abstract

The abundant presence of natural gas reservoirs and ease to convert it with less amount of greenhouse gasses exhaust to useful chemical products make it profitable. Catalytic partial oxidation of methane (POM) is an excellent process for converting methane to various useful chemical compounds and mitigating environmental hazard that are due to the increasing methane concentration in the atmosphere. The most important step in POM is the formation of the synthesis gas. The objective of this study is to utilize BFA as green catalyst support to produce syngas via partial oxidation of methane (POM). BFA was modified using laboratory synthesized La_2O_3 and loaded nickel (Ni) as active metal through the wetness impregnation technique. The Ni/La_2O_3-BFA catalyst was characterized by X-ray diffraction (XRD), scanning electron microscopy (SEM), energy-dispersive X-ray spectroscopy (EDX), thermogravimetric analysis (TGA) and Fourier transform infrared spectroscopy (FTIR) to investigate its suitability for POM reaction. Due to the existence of active Ni species and BFA as the major support, the characterization results indicated greater dispersion of Ni metal over support material, improved thermal stability during high temperature POM reactions, and decreased coke deposition. The presence of various metal oxides such as Al_2O_3, Fe_2O_3, MgO, and SiO_2 in BFA makes it a more suitable support material for POM. The synthesized Ni/La_2O_3-BFA demonstrated superior catalytic activity over La_2O_3-BFA and BFA. The synthesized Ni/La_2O_3-BFA catalyst remained stable for 30 h time on stream (TOS) during POM at 850 ℃. The experimental study demonstrated that the addition of La_2O_3 promoter and active metal Ni to the BFA improved the CH_4 conversion from 55% to 85% and consequently improved H_2/CO ratio from 1.4 to 2.0. The catalytic performance of BFA supported catalyst shows its potential to be adopted for catalytic application, that is a greener, economical, and waste-based alternative to other supported Ni-based catalyst and provide a sustainable solution for decreasing methane emissions.

Keywords: *Partial oxidation of methane; Syngas; Biomass fly ash; La_2O_3; Hydrogen production.*

Table of content

List of Figures

List of Tables

List of Publications

Amin Ul Hasanat, Asif Hussain Khoja*, Majid Ali, Salman Raza Naqvi, Rahat Javaid, Umair Yaqub Qazi and Sami M. ibn Shamsah. Partial oxidation of methane over Ni/La_2O_3 co-supported biomass fly ash (BFA) catalyst for sustainable hydrogen rich syngas production.

Frontiers in Energy Research (IF=4.0). (Under review)

List of Abbreviations

Abbreviation:	Description:
BFA	Biomass fly ash
DRM	Dry reforming of Methane
POM	Partial Oxidation of Methane
SRM	Steam Reforming of Methane
XRD	X-ray Diffraction
SEM	Scanning Electron Microscopy
TGA	Thermogravimetric analysis
FTIR	Fourier Transform Infrared Spectroscopy
EDS	Energy dispersive X-ray
FBR	Fixed bed reactor
TOS	Time of stream
GHG	Greenhouse gases

Chapter 1

Introduction

1.1 Background

Fossil fuels continue to meet the world's growing energy demand. In 2007, US energy usage was at 100 quads, with fossil fuels (natural gas, petroleum, and coal) accounting for 80% of the supply [1]. Meanwhile, primary energy usage increased by 1.3 percent from 2018 levels (2.8 percent). In 2019, it accounted for around 84 percent of global primary energy use. Aside from shale gas production, natural gas (NG) accounts for 36% of total energy consumption. Meanwhile, fossil fuels have maintained their dominance for years [2]. Various combustion methods and developing technologies have a negative impact on our life when it comes to energy utilization. Researchers worked diligently to develop an efficient, non-polluting, and safe technology for fuel combustion. Furthermore, the combustion of fossil fuels is a major producer of greenhouse gases (GHGs) and contribute to climate change by causing global warming (GW).

Since then, crude oil supply has been steadily reduced, and extensive research has been conducted to create clean transportation fuels and alternative resources using various conversion technologies such as biomass to liquid (BTL), coal to liquid (CTL), and gas to liquid (GTL) [3]. Natural gas is a major biomass/fossil fuel reservoir. CH_4 is the abundant constituent of NG (>88%). CH_4 is the most abundant HC on the planet, and it may be found in shale gas, clathrates, landfills, and biomass gas. Furthermore, CH_4 is employed in cooling systems and can be used as a car fuel in compressed form [4]. Renewable and non-renewable energy resources can be used to meet energy demands, however renewable resources are steadily replacing non-renewable resources since renewable fuels have been widely employed as primary energy sources with zero pollution.

Renewable energy sources include wind, solar, hydro, tidal, geothermal, and biomass energy. Biomass is a significant source of renewable energy that is organic in origin. It is the second oldest energy source after the sun. The most common type of biomass used for energy production is woody products. Wood can be burned for heating and cooking purposes alone. Solid waste products are another source of biogas since their combustion creates energy for various uses. Waste to energy power plants continuously burn solid wastes for energy purposes. By rotting or decaying, fungi and bacteria may consume dead animals and plants and turn them into chemical energy in the form of sugar [5].

Bioenergy has been defined as the primary source of renewable energy by the International Energy Agency (IEA). Because of its numerous applications, it is a vital fuel in many countries. It is also employed in transportation fuels and energy generation due to its low GHG emissions [6]. As a result, biomass might be considered an indirect renewable source of solar fuels. It is produced by the combustion of organic materials from plants or animals in biomass-fired power plants. It has significant environmental and economic possibilities, making it a viable alternative to both extremely hazardous and traditional solid fuels [7].

Wood, solid waste, biogas, or any other organic waste is burned in biomass power plants to generate electricity, which is used to power turbines in industries or in households for cooking and heating. It's crucial to know that new biomass-burning technology have been developed to reduce pollution and waste emissions. As a result of the burning of biomass, ash is produced, which can be classified into two types: fly and bottom ashes [8].

In the combustion chamber, biomass bottom ash (BBA) is created by partial or complete oxidation. Sand particles and mineral impurities make up BBA [9]. While biomass fly ash (BFA) is collected outside of the combustion chamber and separated from the gas stream, which is mostly inorganic material with a tiny organic portion (unburnt carbon) [10]. BFA made up of several oxides. The primary elements of BFA are SiO_2, Al_2O_3, Fe_2O_3, K_2O, MgO, MnO, Na_2O, TiO_2, P_2O_5, SO_3, and infrequently CaO [11]. As a result of the existence of metal oxides, which can reduce to metal atoms, it can be utilized as a catalyst. Due to its larger surface area, it can also be

utilized as a supporting material. The pyrolysis of BFA yields hydrogen, a renewable fuel with numerous applications that is extremely significant and used as an energy transporter [12]. Furthermore, Synthesis gas/syngas (H_2/CO) production is a significant initiative for the sustainable development of more competent and ecofriendly biomass resources. Thus, BFA can now be employed as a catalyst in a variety of catalytic reactions. Given the increasing accessibility of NG in recent decades, methane conversion to various transportation fuels and other petroleum/liquid products has been greatly anticipated [13].

As indicated by the literature, several researchers have focused on various petroleum alternatives as energy sources, making CH_4 an appealing and powerful option for this purpose [14]. In general, CH_4 conversion can be categorized into direct and indirect paths, while the second paths of CH_4 conversion to synthesis gas is more cost-effective and feasible [15]. H_2/CO is a key precursor to produce a variety of useful chemicals, including ammonia (for urea synthesis), methanol, Fischer Tropsch fuels (liquid fuels transportable via existing pipeline systems) [16], and the synthesis of various aromatic and aliphatic hydrocarbons for various applications [17].

One of the most important and essential paths to conversion is reforming [18]. As a result, reforming technologies for methane conversion have been developed. In the presence of catalysts, steam reforming of methane (SRM), dry reforming (DRM), and partial oxidation of methane (POM) are the most often utilized syngas generation technologies. SRM is one of the most used syngas reforming methods, however it is extremely endothermic (needs superheated steam) and demands a higher initial investment [19]. However, due to the production of GHGs (CH_4 and CO_2) and coke deposition, it was illegal to synthesis syngas by DRM and SRM in the past decades [20].

Partially oxidation of methane (POM) is appropriate and beneficial technology for syngas production among other reforming technologies. As a result, considerable research has been done on it, and a variety of catalyst systems for the POM reaction have been devised, including nickel (Ni), cobalt (Co), copper (Cu), iron (Fe), rhenium (Re), palladium (Pd), platinum (Pt), and others [21].Because of their various features, Ni-containing catalysts were produced in this study utilizing BFA and La_2O_3 as

support material and promotor respectively, which will be addressed briefly in the next section.

1.2 Problem Statement

Even though partial oxidation (R1) is an effective process for synthesizing syngas, it has some drawbacks, which prompted us to carry out this research. Catalysts for syngas generation can be made easily with a variety of commercially available salts and support materials, the complication, waste produced during synthesis, and the cost of such a catalyst system is a major barrier[22]. Research is being carried out to synthesize catalyst or catalyst support from waste material that is economical, greener, easy to synthesize and renewable source. The biomass fed power plants generate enormous amounts of fly ash and bottom ash, and their discarding is a major concern. Biomass fly ash (BFA) has some notable structural features and contains numerous metal oxides, making it appropriate for use as a catalyst or catalyst support material in POM as well as other reforming applications.

$$CH_{4(g)} + \frac{1}{2}O_2 \rightarrow CO_{(g)} + 2H_{2(g)} \qquad \text{(R 1)}$$

Furthermore, DRM and SRM, are more ideal for the synthesis of diesel or other liquid hydrocarbons via the Fischer Tropsch process however it is difficult to achieve H_2/CO molar ratios greater than 1 with these processes. Because of the high exothermicity of the POM reaction and the presence of active metal in the catalyst result in the formation of hot spots on the surface of the catalyst that reduce the catalytic activity of catalysts by sintering or coke deposition, reducing the catalytic activity of catalysts.

1.3 Research Hypothesis

For the generation of syngas, the POM reaction has been increasingly utilized, and researchers have developed many catalyst systems. The Future of POM relies heavily on catalyst advancements. Transition metal catalysts have better properties and advantages in terms of resistance to coke deposition than Ni catalysts, however, this is only possible at higher temperatures due to the acidic nature of the supporting

materials. Coke deposition can be avoided by high metal loading, however noble metals are quite expensive. Metal carbides or a bimetallic catalytic system can be used to solve the problem. It is important to minimize the cost of synthesizing catalysts.

Therefore, we used POM for syngas production in the presence of nickel loaded over biomass fly ash as support and promoted with lanthanum oxide. BFA has been identified to be a mixture of metal oxides including Al_2O_3, $CaSO_4$, $CaCO_3$, Fe_2O_3, and SiO_2 [23]. Lanthanum oxide has been added as a promoter to boost the stability of the catalyst and provide better dispersion of nickel over BFA.

1.4 Objectives of Study

The research presented in this thesis focuses on a biomass fly ash-derived nickel base catalyst for partial oxidation of methane. The main topics of this research are the performance of biomass fly ash generated catalyst, catalytic activity, methane conversion, hydrogen selectivity, hydrogen yield, carbon monoxide selectivity and syngas ratio. The experimental work done in this study is completely consistent with the literature. This research study's main goal is:

- To synthesize and characterize BFA supported Ni-based catalyst promoted with La_2O_3 for POM process.
- To investigate the catalytic activity and stability of Ni/ La_2O_3-BFA catalyst in fixed bed reactor.

1.5 Scope of Study

The synthesis and analysis of catalysts is the cornerstone of reaction and process engineering. After collecting biomass fly ash from a nearby biomass-fired generating station, the BFA sample was prepared for the catalyst's support material. Lanthanum oxide was synthesized through the sol-gel method. The incipient wetness impregnation method was used to create a final catalyst loaded with active metal nickel and La_2O_3 as a promoter over BFA support. The synthesized catalyst was investigated, tested, and analysed by a variety of methods. The in-depth study of partial oxidation of methane discloses that the process hinges on a variety of factors that type of support material, active metal, type of promoter, catalyst’s preparation method, reaction

mechanism and experimental parameters. The scope of the research is presented in Figure 1-1

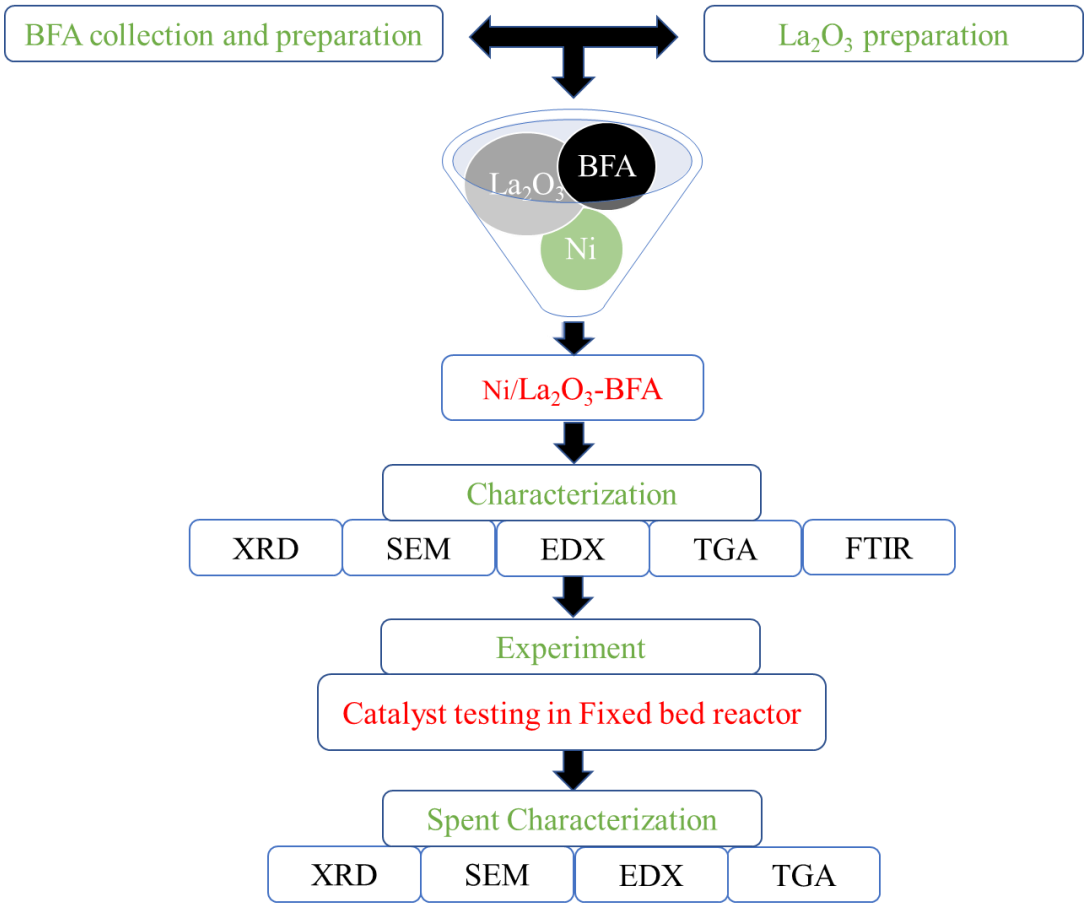

Figure 1-1 Steps involved in the research scope.

1.6 Flow chart of thesis

The research was first intended to examine how to manage BFA in a sustainable manner rather than dumping it in landfills. BFA samples were cleaned and prepared and then impregnated with nickel and La_2O_3 in the material preparation and characterization section. The synthesized catalyst was characterized by characterization techniques such as XRD, TGA, SEM, EDS and FTIR. The synthesised and characterised final catalyst was evaluated in FBR at the reaction temperature of about 850 °C. The data of the results were extensively discussed in the results and discussion section. The final section discusses how to effectively use BFA as a catalytic material and how adding La_2O_3 and Ni to BFA improves the catalyst's stability and catalytic activity.

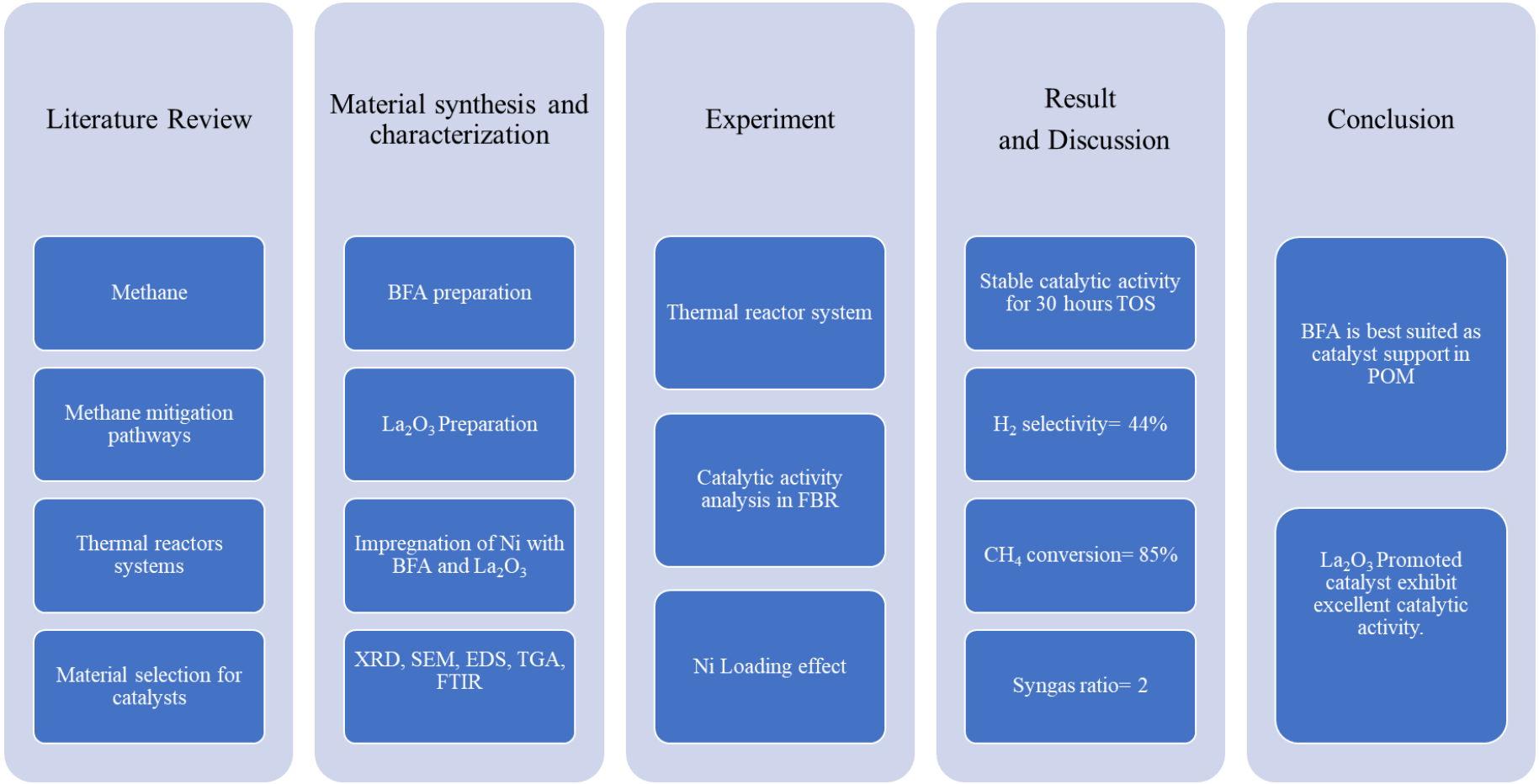

Figure 1-2 Thesis flow diagram

References

[1] N.A.o. Sciences, N.A.o. Engineering, N.R. Council, America's Energy Future: Technology and Transformation, The National Academies Press, Washington, DC, 2009.

[2] P.N.Y. Yek, Y.W. Cheng, R.K. Liew, W.A. Wan Mahari, H.C. Ong, W.-H. Chen, W. Peng, Y.-K. Park, C. Sonne, S.H. Kong, M. Tabatabaei, M. Aghbashlo, S.S. Lam, Progress in the torrefaction technology for upgrading oil palm wastes to energy-dense biochar: A review, Renewable and Sustainable Energy Reviews, 151 (2021) 111645.

[3] H. Nourbakhsh, J. Rahbar Shahrouzi, H. Ebrahimi, A. Zamaniyan, Experimental study of ultra-rich thermal partial oxidation of methane using a reticulated porous structure, International Journal of Hydrogen Energy, 45 (2020) 12298-12307.

[4] S.A. Solarin, I. Ozturk, The relationship between natural gas consumption and economic growth in OPEC members, Renewable and Sustainable Energy Reviews, 58 (2016) 1348-1356.

[5] R. Slade, A. Bauen, Micro-algae cultivation for biofuels: Cost, energy balance, environmental impacts and future prospects, Biomass and Bioenergy, 53 (2013) 29-38.

[6] R. Quadrelli, S. Peterson, The energy–climate challenge: Recent trends in CO_2 emissions from fuel combustion, Energy Policy, 35 (2007) 5938-5952.

[7] M.S. Ghayal, M.T. Pandya, Microalgae Biomass: A Renewable Source of Energy, Energy Procedia, 32 (2013) 242-250.

[8] E. Akkaya, ANFIS based prediction model for biomass heating value using proximate analysis components, Fuel, 180 (2016) 687-693.

[9] B. Carrasco, N. Cruz, J. Terrados, F.A. Corpas, L. Pérez, An evaluation of bottom ash from plant biomass as a replacement for cement in building blocks, Fuel, 118 (2014) 272-280.

[10] A. Fuller, J. Maier, E. Karampinis, J. Kalivodova, P. Grammelis, E. Kakaras, G. Scheffknecht, Fly Ash Formation and Characteristics from (co-)Combustion of an Herbaceous Biomass and a Greek Lignite (Low-Rank Coal) in a Pulverized Fuel Pilot-Scale Test Facility, Energies, 11 (2018) 1581.

[11] R. Rajamma, R.J. Ball, L.A.C. Tarelho, G.C. Allen, J.A. Labrincha, V.M. Ferreira, Characterisation and use of biomass fly ash in cement-based materials, Journal of Hazardous Materials, 172 (2009) 1049-1060.

[12] C. Quan, S. Xu, C. Zhou, Steam reforming of bio-oil from coconut shell pyrolysis over Fe/olivine catalyst, Energy Conversion and Management, 141 (2017) 40-47.

[13] L. Zhang, Y. Hu, W. Xu, C. Huang, Y. Su, M. Tian, Y. Zhu, H. Gong, X. Wang, Anti-coke $BaFe_{1-x}Sn_xO_{3-\delta}$ Oxygen Carriers for Enhanced Syngas Production via Chemical Looping Partial Oxidation of Methane, Energy & Fuels, 34 (2020) 6991-6998.

[14] A.H. Khoja, M. Tahir, N.A.S. Amin, A. Javed, M.T. Mehran, Kinetic study of dry reforming of methane using hybrid DBD plasma reactor over La_2O_3 co-supported $Ni/MgAl_2O_4$ catalyst, International Journal of Hydrogen Energy, 45 (2020) 12256-12271.

[15] S. Pei, M.S. Kleefisch, T.P. Kobylinski, J. Faber, C.A. Udovich, V. Zhang-McCoy, B. Dabrowski, U. Balachandran, R.L. Mieville, R.B. Poeppel, Failure mechanisms of ceramic membrane reactors in partial oxidation of methane to synthesis gas, Catalysis Letters, 30 (1994) 201-212.

[16] T.J. Siang, A.A. Jalil, A.A. Abdulrasheed, H.U. Hambali, W. Nabgan, Thermodynamic equilibrium study of altering methane partial oxidation for Fischer–Tropsch synfuel production, Energy, 198 (2020) 117394.

[17] Q. Bkour, F. Che, K.-M. Lee, C. Zhou, N. Akter, J.A. Boscoboinik, K. Zhao, J.T. Gray, S.R. Saunders, M. Grant Norton, J.-S. McEwen, T. Kim, S. Ha, Enhancing the partial oxidation of gasoline with Mo-doped Ni catalysts for SOFC applications: An integrated experimental and DFT study, Applied Catalysis B: Environmental, 266 (2020) 118626.

[18] V.A. Tsipouriari, X.E. Verykios, Carbon and Oxygen Reaction Pathways of CO2 Reforming of Methane over Ni/La_2O_3 and Ni/Al_2O_3 Catalysts Studied by Isotopic Tracing Techniques, Journal of Catalysis, 187 (1999) 85-94.

[19] S. Sengodan, R. Lan, J. Humphreys, D. Du, W. Xu, H. Wang, S. Tao, Advances in reforming and partial oxidation of hydrocarbons for hydrogen production and fuel cell applications, Renewable and Sustainable Energy Reviews, 82 (2018) 761-780.

[20] T.T.P. Pham, K.S. Ro, L. Chen, D. Mahajan, T.J. Siang, U.P.M. Ashik, J.-i. Hayashi, D. Pham Minh, D.-V.N. Vo, Microwave-assisted dry reforming of methane for syngas production: a review, Environmental Chemistry Letters, 18 (2020) 1987-2019.

[21] F.B. Passos, E.R. Oliveira, L.V. Mattos, F.B. Noronha, Effect of the support on the mechanism of partial oxidation of methane on platinum catalysts, Catalysis Letters, 110 (2006) 161-167.

[22] C. Zhao, L. Yang, S. Xing, W. Luo, Z. Wang, P. Lv, Biodiesel production by a highly effective renewable catalyst from pyrolytic rice husk, Journal of Cleaner Production, 199 (2018) 772-780.

[23] M. Assad Munawar, A. Hussain Khoja, M. Hassan, R. Liaquat, S. Raza Naqvi, M. Taqi Mehran, A. Abdullah, F. Saleem, Biomass ash characterization, fusion analysis and its application in catalytic decomposition of methane, Fuel, 285 (2021) 119107.

Chapter 2
Literature Review

2.1 Methane Overview

Methane is the main component of natural gas that is in abundance and is going to outlast oil by a margin of around 60 years [1]. Maximum natural gas reservoirs are located offshore or farthest from the industrial complex so they cannot be transported through pipelines and its liquification for shipping through the ocean is expensive[2]. About 140 billion cubic meters of natural gas is flared globally resulting in the waste of important hydrocarbon and global warming due to increased GHG emissions [3].

The growing population has increased the rate of waste generation thrown into landfills resulting in more methane production as a by-product and causing an environmental issue [4]. Methane used directly for burning produces NOx and SOx which is hazardous for the environment [5] and constitute a major part of GHG. Keeping the environment and health factor in focus enormous research is going on to convert methane into liquid fuel or higher hydrocarbons[6] that are more valuable and cleaner.

Researchers studied the direct oxidation of methane to methanol, formaldehyde, propanol, benzene etc. but the result was not promising enough[7]. Of particular interest in this respect is the partial oxidation of methane to synthetic gas or syngas which is the building block for valuable fuels and chemicals[8]. Synthetic gas is the feedstock for oxygenates as well as the making of liquid and solid hydrocarbon by Fischer-Tropsch (FT) syntheses [9].

The methane conversion has gained much interest via the reforming techniques, such as dry reforming of methane (DRM)[10], steam reforming of methane (SRM) [11], bi-reforming, try reforming of methane and partial oxidation of methane (POM) [12]. Steam reforming (SRM) is preferred for the industrial production of syngas which is then used to produce ammonia or methanol [13] but it is an energy-

intensive process so more energy-efficient alternatives are sought to produce synthesis gas.

2.2 Methane Mitigation Pathways

Global consumption of fossil fuel due to the increasing population has caused continuous growth of CH_4 concentration in the atmosphere which has 25 times more global warming potential than CO_2. The researchers are trying to develop efficient strategies to reduce CH_4 emissions to the atmosphere. Several routes are suggested which includes (1) Promoting energy conservation and increasing energy efficiency, but it requires high capital investment to install energy-saving devices. (2) Replacing fossil fuel with renewable energy but the renewable is not mature enough to replace fossil fuel technology. (3) Methane capture and utilization is a technique used to convert methane into green fuel, currently, methane is used as feedstock to produce syngas which is the building block for many chemicals and can be used directly as a green fuel. Therefore, chemical recycling of CH_4 as presented in Figure 2-1 is an attractive alternative to reduce CH_4 emission into the atmosphere and its conversion to renewable fuels is the best strategy for reducing CH_4 emissions.

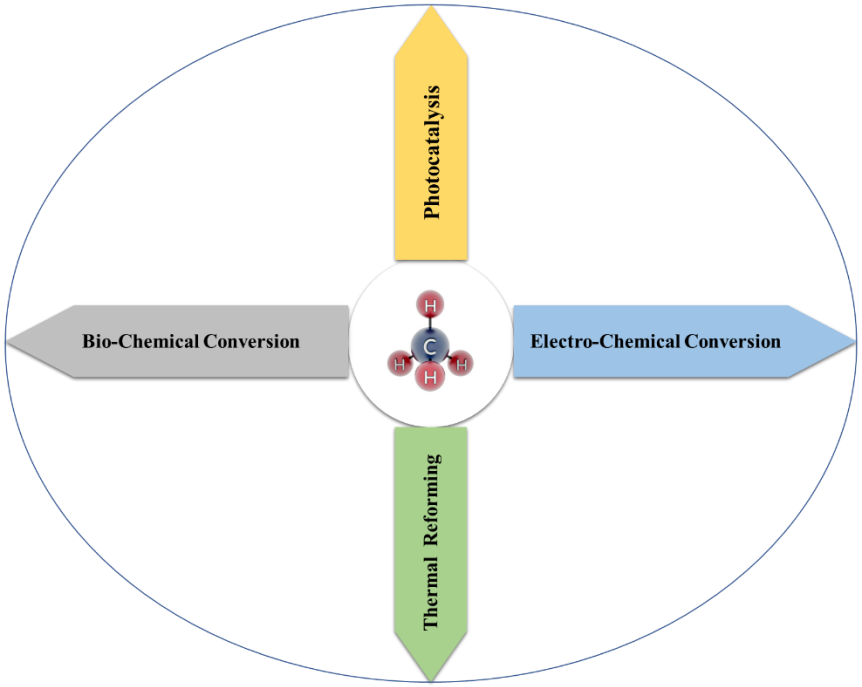

Figure 2-1 Methane mitigation pathways

2.3 Reforming Technologies for CH_4 Conversion To Green Fuel

Research and development (R&D) are ongoing to develop an effective method to convert CH_4 into green fuel. Currently, different technologies are used for CH_4 conversion to green fuel. However, in the following section, we will concentrate on the reforming processes for methane conversion to syngas, as described in Figure 2-2.

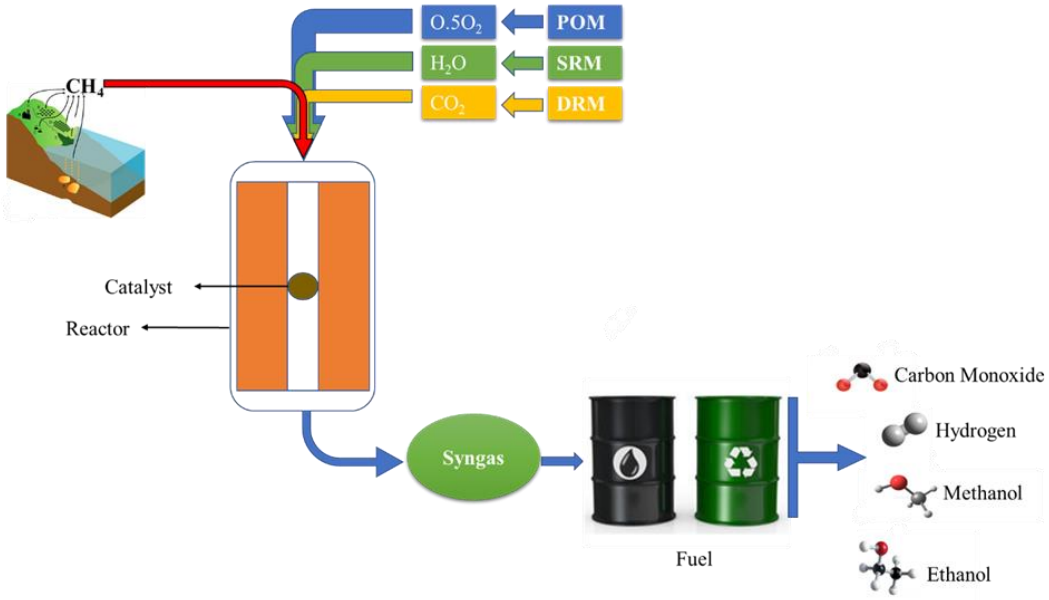

Figure 2-2 Conversion of CH_4 into green fuel through reforming processes

2.3.1 Steam Reforming of Methane

Steam reforming of methane (SRM) is the most developed and effective method used worldwide to produce hydrogen from methane. In United State, about 95% of hydrogen is produced by SRM[14]. In SRM methane and steam reaction (R 2) are assisted by catalyst at a temperature above 800 °C and pressure of 2 MPa. However, SRM has a disadvantage of being highly exothermic, CO_2 emissions, high operating cost, boudoir reaction (R 3) and coke formation due to methane decomposition (R 4) [15, 16].

$$CH_4 + H_2O = CO + 3H_2 \qquad \Delta H_{298} = 206\ kJ\ mol^{-1} \qquad \text{(R 2)}$$

$$2CO = C + CO_2 \qquad \Delta H_{298} = -172\ kJ\ mol^{-1} \qquad \text{(R 3)}$$

$$CH_4 = C + 2H_2 \qquad \Delta H_{298} = 206\ kJ\ mol^{-1} \qquad \text{(R 4)}$$

2.3.2 Dry Reforming of Methane

Dry reforming uses economical CO_2 instead of steam as an oxidizing agent to produce H_2 though (R 5). Its major advantage is its potential to reduce the carbon footprint of power and industrial plants. However, its usage is limited in chemical industries because of the low H_2/CO ratio due to reverse WGS reaction (R 6), endothermic reaction that makes it a highly energy-intensive process and catalyst deactivation due to coke formation [17-19].

$$CH_4 + CO_2 = 2CO + 2H_2 \qquad \Delta H_{298} = 247kJ\ mol^{-1} \qquad \text{(R 5)}$$

$$H_2 + CO_2 \leftrightarrow CO + H_2O \qquad \Delta H_{298} = 41.2kJ \cdot mol^{-1} \qquad \text{(R 6)}$$

2.3.3 Bi Reforming of Methane

The bi-reforming process is the combination of SRM and DRM utilizing steam and CO_2 for reforming methane to produce syngas (R 7). It is a promising alternative to SRM and DRM because of CH_4 and CO_2 mitigation, higher catalytic stability, flexible H_2/CO ratio that is suitable for the Fischer Tropsch process and lower carbon deposition. However, it has limitations of high operating cost and catalyst synthesis to withstand steam-rich operation for a longer duration [20-24]

$$3CH_4 + CO_2 + 2H_2O = 4CO + 8H_2 \qquad \Delta H_{298} = 151kJ \cdot mol^{-1} \qquad \text{(R 7)}$$

2.3.4 Tri Reforming of Methane

Tri-reforming of methane is the reforming of methane in the presence of H_2O, CO_2, and O_2. This process is a combination of POM, SRM, and DRM reactions. The uniqueness associated with the tri-reforming of methane is the direct utilization of flue gases from fossil fuel power plants [25] for reforming methane to syngas thus

eliminating the cost required for pure CO_2. Carbon formation can be hindered due to the existence of steam and oxygen. Combination three of reaction result in higher energy efficiency. Required H2/CO ratio can be obtained by adjusting the feed ratio [26]. However, the tri-reforming of methane has the demerits of SO_x NO_x emissions and the inability of catalysts to withstand the harsh reaction environment [27]

2.3.5 Auto-Thermal Reforming of Methane

Auto-thermal reforming is a combination of different reactions such as the combustion of methane, POM and SRM. ATR start with methane combustion reaction (R 8) followed by SRM and POM. ATR reactors consist of a combustion zone and reforming zone having temperatures of about 1927 °C and 900-1199 °C respectively. ATR can overcome the problem of the hot spot in POM and H_2/CO ratio in SRM thus a more advantageous and economical route to produce syngas. However, feed is lost by the side reaction of methane combustion.

$$CH_4 + O_2 = CO_2 + 2H_2O \qquad \Delta H_{298} = -801 kJ \cdot mol^{-1} \qquad \text{(R 8)}$$

2.3.6 Partial Oxidation of Methane

In POM syngas is produces through partial oxidation of methane (R 9). However other reactions are also taking place as shown in Table 2-1. It is a promising approach to syngas production that have many advantages such as the exothermic nature of the reaction, production of syngas with a ratio of 2:1 that can be used for liquid fuel production via the Fischer-Tropsch synthesis process [28, 29]. From an energy and economic perspective, POM is efficient because it allows the use of smaller reactors, lower energy utilization and a quick reaction rate [30-32]. Despite the above advantages, POM has a demerit of hot spot formation that results in catalyst sintering and deactivation [32-34].

$$CH_4 + \frac{1}{2}O_2 = CO_2 + 2H_2 \qquad \Delta H_{298} = -36kJ \cdot mol^{-1} \qquad \text{(R 9)}$$

Table 2-1 Reactions involved in POM [54]

Reactions	ΔH_{298} =-36 kJ mol^{-1}
$CH_4 + 0.5O_2 = CO + H_2$	-36
$CH_4 + 2O_2 = CO_2 + 2H_2$	-802
$CH_4 + H_2O = CO_2 + 3H_2$	206
$CH_4 + 2H_2O = CO_2 + 4H_2$	165
$CH_4 + CO_2 = 2CO + 2H_2$	247
$H_2O + CO = CO_2 + H_2$	-41

2.3.6.1 Chemical Looping Partial Oxidation of Methane

To remove the need for pure oxygen in POM chemical looping, partial oxidation of methane is used, as illustrated in Figure 2-3. In chemical looping POM, the pure oxygen required is provided by a lattice oxygen carrier. Lattice oxygen carriers react with methane to produce syngas. The reduced lattice oxygen carrier is again reoxidized by air in the additional reactor at elevated temperatures. In Chemical looping POM methane react with lattice oxygen instead of pure oxygen thus reducing the explosion risk and cost by eliminating the need for an air separation unit [35, 36]. However, it has some demerits such as the oxides oxygen carriers results in the complete combustion of methane instead of partial oxidation, carrier attrition and difficulty in scaling up the reactor [37, 38]

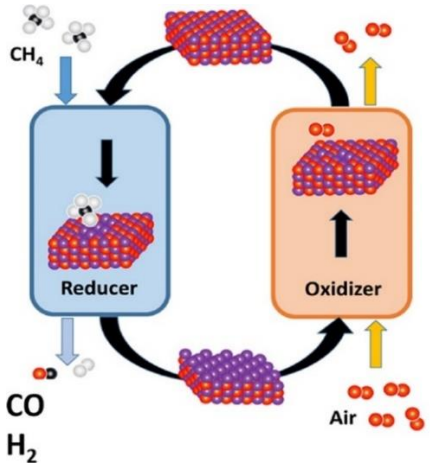

Figure 2-3 Chemical looping POM configuration [48]

2.3.6.2 Thermodynamics of POM

POM is presented in Figure 2-4 schematically along with thermodynamic information. POM is an important reforming process that has thermodynamic advantages over other reforming processes such as Mild exothermicity of POM enable us to design economical reactor to heat which can further be coupled with endothermic DRM or SRM to increase its energy efficiency, the H_2/CO ratio of around 2 that avoid the removal of valued hydrogen and is ideal for downstream processes, extremely low CO_2 is produced in POM that should be removed before using syngas for downstream processes and POM does not require an expensive large amount of superheated steam, however, for pure oxygen supply oxygen separator is required that is expensive.

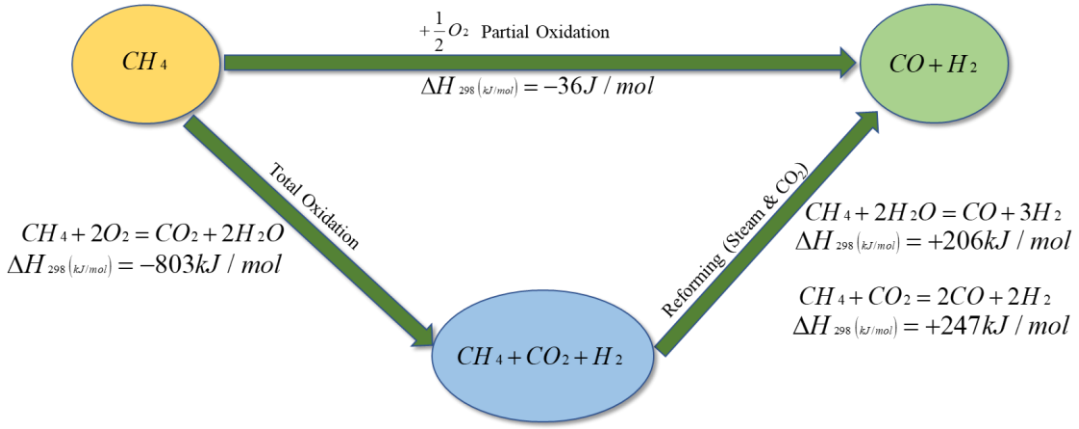

Figure 2-4 Thermodynamic pathways for partial oxidation of methane

POM to syngas proceeds in two steps. In first step methane combustion (Eq 9) occurs while in the second step the remaining methane react with the products of first reaction to produce syngas (R 10, R 11, R 12)

$$2CH_4 + O_2 = 1.5CH_4 + 0.5CO_2 + 2H_2O \quad \text{(R 10)}$$

$$0.5CH_4 + 0.5CO_2 = CO + H_2 \quad \text{(R 11)}$$

$$CH_4 + H_2O = CO + H_2 \quad \text{(R 12)}$$

$$2CH_4 + O_2 = 2CO + 4H_2 \quad \text{(R 13)}$$

Based on the above reactions the 3D data plots, Figure 2-5 shows high temperature is favorable for methane conversion, hydrogen, and carbon monoxide selectivity's because at a temperature lower than 450K there is no conversion as the kinetic barriers cannot be breached while high pressure is unfavorable to reforming reactions because it further moves it away from syngas formation and favors CO_2 and H_2O.

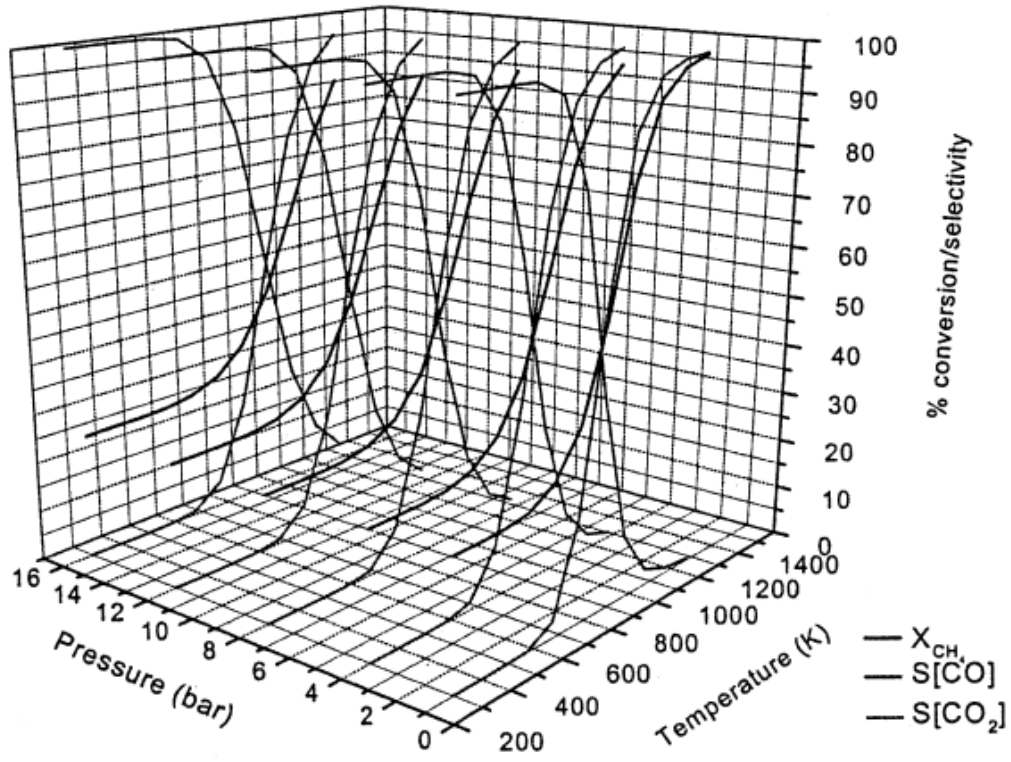

Figure 2-5 Thermodynamic calculation of POM to syngas, Methane conversion, H_2 and CO selectivity's w.r.t pressure and temperature [25]

2.4 Criteria for Selecting Methane Reforming Process

The most important factor affecting the selection of the methane reforming process among different processes is the syngas ratio (H_2/CO) Because the syngas ratio determines the process by which the syngas will be further utilized. The required syngas ratio for the Fischer Tropsch process, for example, is between -2.5 while for ammonia production it is 3 or greater. However, each process has merits and demerits depending upon the reaction mechanism, operating conditions, feed, and catalyst.

2.5 Classification of Reactors for POM

Designing a reactor is an engineering approach to increase the efficiency of CH_4 conversion to green fuel by POM. Different factors such as the material of construction, heat exchange, flow characteristics, and membrane used effects the reactor performance therefore play important role in the design of a reactor. In literature, the reactors are classified into different categories based on the type of bed, the membrane used, phases involved and operational mode.

2.5.1 Fixed Bed Reactor

Fixed bed reactors are commonly used for POM. They are heterogeneous reaction systems that are easy to set up and maintain. Fixed bed reactors consist of vertical cylindrical shells made of quartz or steel in which reactants gases flow by gravity. Inside the reactor, there is a heating zone that has a fixed bed for catalyst and is heated by an electric furnace. A controlled flow of gases through the flow meter is fed from the top to the reactor and where they react over the catalyst bed to form synthesis gas and passed through the condenser to remove vapour content before being collected at the bottom. The temperature required for POM is controlled by the process's controller while the temperature at the catalyst bed is measured by a thermocouple in a fixed bed reactor. Usually, the temperature required without a catalyst is (1200 -1500) °C [39] while the introduction of catalyst reduces the temperature to (700-850) °C, therefore the development of catalysts is of utmost importance in fixed bed reactor.

Fixed bed reactor can be classified into vertical or horizontal fixed bed reactor based on the orientation of reactor vessel as shown in Figure 2-6. However vertical fixed bed reactor is preferred due to various advantages such as suitableness for mixed flow and low space requirement. Horizontal fixed bed reactor used only when the reaction is strongly favored by horizontal fixed bed reactor.

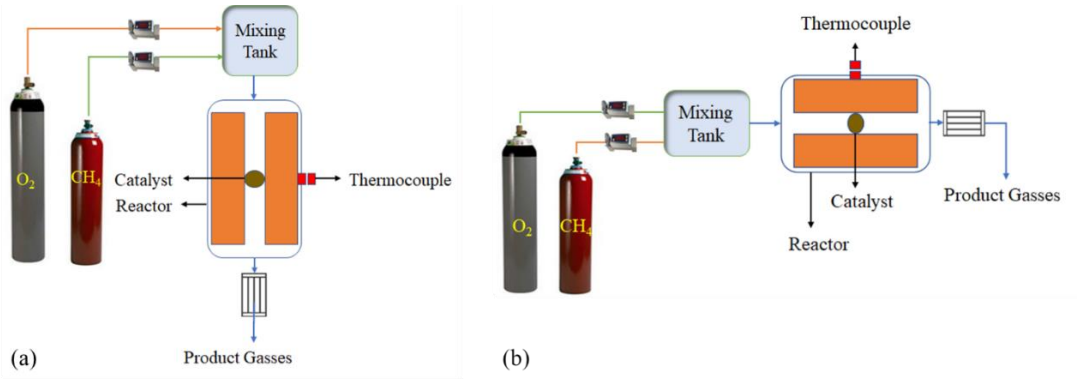

Figure 2-6 (a) Vertical fixed bed reactor (b) Horizontal fixed bed reactor

Fixed bed reactor possesses various advantages such as immobilized catalyst supported over fixed support, continuous operation without the need for catalyst separation thus more economical, and unrestricted flow rate, better conversion per unit catalyst mass, reduce pressure drop, that enables fixed bed reactor operation more efficient and economical. However, the high reaction rate in POM creates a large temperature gradient which results in the hotspots [40] in the packed bed, causing experimental findings to be inaccurate [41]. This prevents scaling up of the reactor for industrial applications.

In a fixed bed reactor methane conversion and syngas ratio mostly depend on non-tangible factors such as temperature, pressure, and gas velocities. The tangible factors that can affect the performance are the catalyst and the tube material[42]. The fixed bed reactors along with reaction parameters, tube material, methane conversion and syngas ratio are summarized in Table 2-2.

Table 2-2 Summary of fixed bed reactor used in POM

Reactor	**Dimension**	**T (°C)**	**Tube Material**	**XCH_4 (%)**	**Ref**
Fixed bed reactor		550	Quartz	30	[43]
Fixed bed reactor	Di=10 mm	700	Quartz	55	[44]
Fixed bed reactor	Di=6 mm L=600 mm	700	Quartz	86.4	[45]
Fixed bed reactor	Di=8 mm L=700mm	700	Quartz	72	[46]
Fixed bed reactor	Di=10 mm L=700mm	700	Quartz	87	[30]
Fixed bed reactor	Di=8 mm	700		88	[47]
Fixed bed reactor	Di=9 mm	800	Quartz	91	[48]
Fixed bed reactor		800	Quartz	80	[49]
Fixed bed reactor	Di=10 mm	800	Quartz	92	[50]
Fixed bed tabular reactor	Di=9 mm L=300mm	800	Hastelo X tube	80	[51]
Fixed bed reactor		800	Quartz	78	[52]
Fixed bed reactor	Di=13 mm L=750mm	900	Quartz	96	[53]

2.5.2 Fluidized Bed Reactor

Fluidized bed reactors are heterogeneous reaction systems in which catalysts are fluidized [54] therefore named fluidized bed reactors. The fluidized bed reactor system consists of a reactor tube that has initially a catalyst in a fixed bed configuration with motionless catalyst particles. When the inlet gas velocity increases the particle start motion and becomes fluidized known as fluidization configuration. The fluidized bed is heated by an electric furnace whose temperature is measured by a thermocouple and controlled by a process controller. Mass flow controllers were used to controlling the reactant gases that are fed from the bottom where they pass through catalyst and react to form product gases. The product gases then pass through the condenser to remove the moisture and are further analyzed by GC as presented in Figure 2-7.

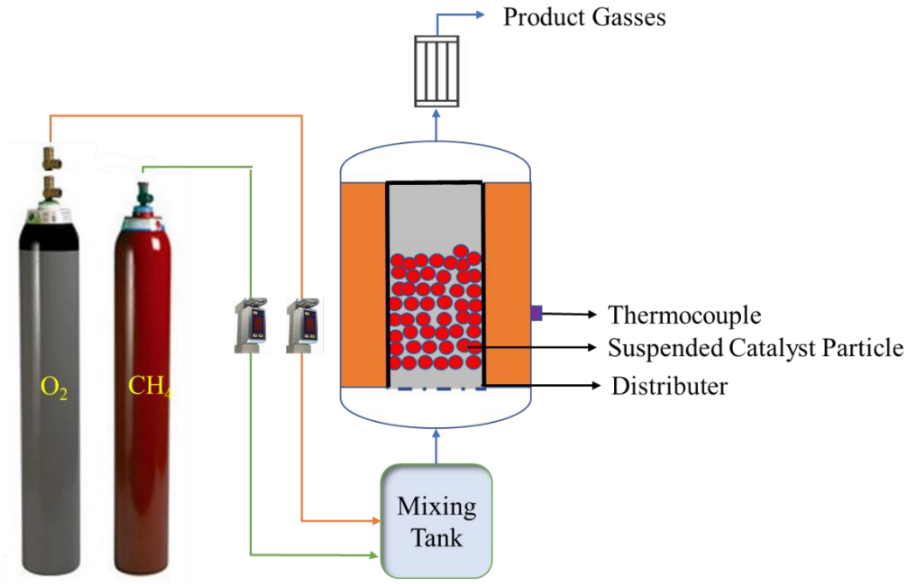

Figure 2-7 Fluidized bed reactor configuration

Catalyst particles type play an important role in the fluidization phenomenon. Particle are classified into group A, B, C and D based on size of particle and difference of density between gas and particle as presented in Figure 2-8.

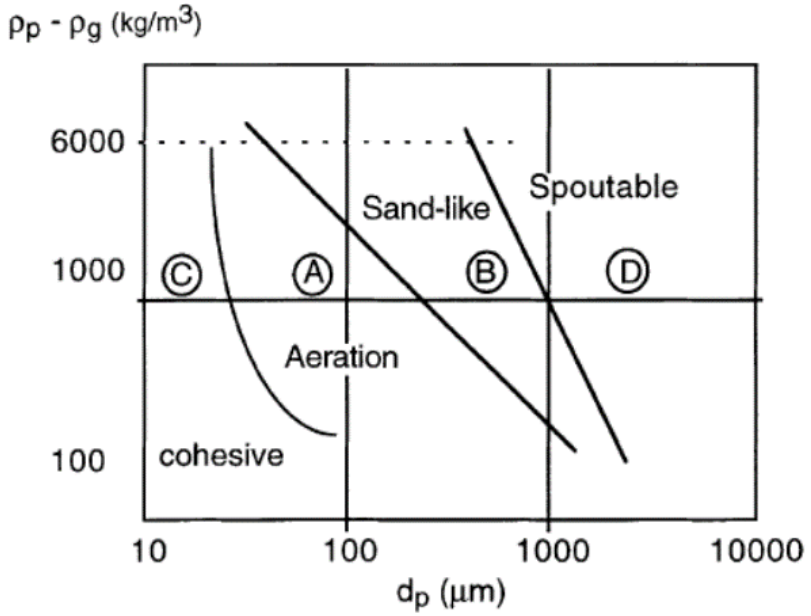

Figure 2-8 Particle classification by Geldart [55]

Fluidization of catalyst particles is achieved when the gravitational force over the catalyst particle becomes equal to the drag exerted on the catalyst particle due to the pressure drop by rising inlet gasses. The fluidization of the particle is dependent on the inlet gas velocity known as fluidization velocity that can be calculated by (Eq 1) and (Eq 2). The relation between the pressure drops and fluidization velocity is presented in Figure 2-9.

When Rep < 10, the minimum fluidization velocity u_{mf} can be calculated as

$$U_{mf} = \frac{(\emptyset_s d_p)^2}{150}\frac{(\rho_s - \rho_g)}{\mu}\left(\frac{\varepsilon_{mf}^3}{1-\varepsilon_{mf}}\right) \qquad \text{Eq 1}$$

When Rep > 1000, the minimum fluidization velocity u_{mf} can be calculated as

$$U_{mf} = \left[\frac{\emptyset_s d_p}{1.75}\frac{(\rho_s - \rho_g) g \varepsilon_{mf}^3}{\rho_g}\right]^{1/2} \qquad \text{Eq 2}$$

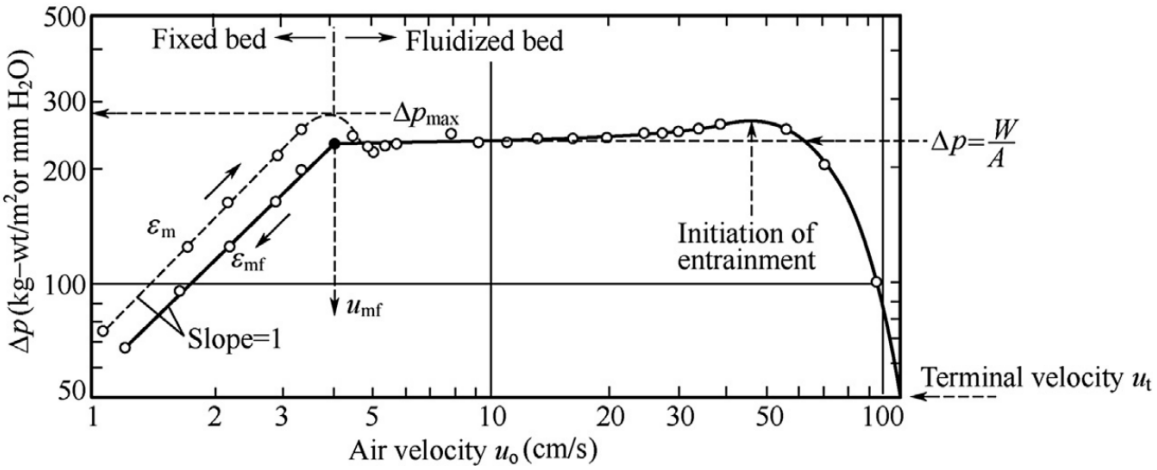

Figure 2-9 Fluidization velocity vs pressure drop relationship [55]

Fluidized bed reactor advantages include a fluidized catalyst that acts as heat carrier and ensure homogenous temperature [55] throughout the reactor thus solving the problem of hot spot creation within the catalyst bed, the temperature can be easily controlled, heat and mass transfer is enhanced by fluidization, favorable conditions are formed by catalyst particle circulation for carbon burning over the oxygen-rich zone that limits carbon deposition [60], fluidization increase methane activation by regenerating active sites[56]. These reactors can handle a large amount of feed and catalysts due to periodic addition and removal. However, it has some cons as well such as non-uniform distribution of gas, solid particle back mixing, gas bypassing and transfer of catalyst particles. The dimensions, reaction parameters, and methane conversion of a fluidized bed reactor are summarized in Table 2-3.

Table 2-3 Summary of Fluidzed bed reactor used in POM

Reactor	**Dimension**	**T (°C)**	**XCH_4 (%)**	**Remarks**	**Ref**
Fluidized bed reactor	Di=20 mm H=750 mm	700	74	Fluidized beds necessitate catalysts having supports with high mechanical strength.	[57]
Bubbling fluidized bed reactor	Di=30 mm H=235 mm	850	90	If the catalyst particles are prevented from entering the reactor's colder zone, more conversion and selectivity can be attained.	[58]
Fluidized bed reactor	Di=22 mm H=350 mm	800	92	In a fluidized bed reactor, isothermal operation and performance near thermodynamic equilibrium could be attained.	[41]
Fluidized bed reactor	Di=24 mm H=250 mm	700		In industrial processes, back reactions restrict reactor scaling, not reaction rates.	[55]
Fluidized bed reactor	Di=20 mm H=750 mm	750	86	To achieve the required syngas ratio, CO_2 reforming, and POM can be coupled.	[59]
Bubbling fluidized bed reactor	Di=50 mm H=750 mm	800	96	Due to particle back mixing and mass transfer constraints, the catalyst remained in a reduced form.	[60]
Bubbling fluidized bed reactor	Di=50 mm H=500 mm	800		Carbon deposition in the bubbling fluidized reactor is minimum as the catalyst is continuously regenerated.	[61]

2.5.3 Membrane Reactor for POM

A membrane reactor is another widely used reactor for POM that consists of an oxygen-permeable membrane, therefore, named a membrane reactor. The permeable membrane is integrated with the catalyst thus combining the separation of oxygen from the air on one side and providing pure oxygen for methane oxidation over the catalyst surface on the other side in one unit as presented in Figure 2-10. Membrane reactors solve the two main problems of POM such as reaction and separation can be carried out simultaneously in one compact reactor system thus reducing cost and uniform permeation of oxygen through membrane prevent the formation of a hot spot by uniform temperature distribution that prevents overheating of catalyst inlet and reduce the safety risk [62]. However, it has the difficulty in maintaining stability while reducing CO_2, CO, H_2, H_2O and CH_4.

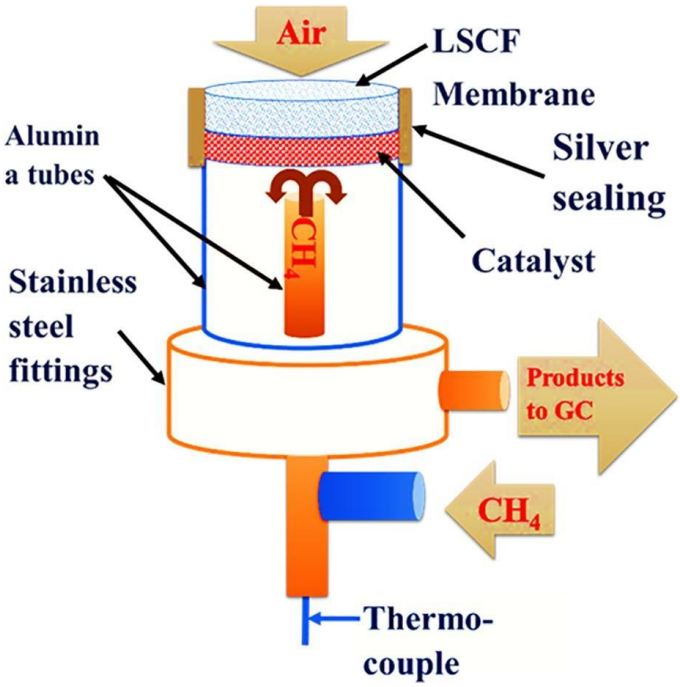

Figure 2-10 Membrane reactor setup [69]

Membrane reactors are classified based on the shape of the membrane. The most common types are tabular and disk membrane reactors as presented in Figure 2-11 each having its merit and demerits. Disk membrane is less expensive with easy fabrication however it has lower mechanical strength that makes its scaling up difficult [63, 64]. The tabular membrane has better stability than the disk membrane but is

expensive and the geometry makes the cleaning of the membrane much more difficult [65, 66].

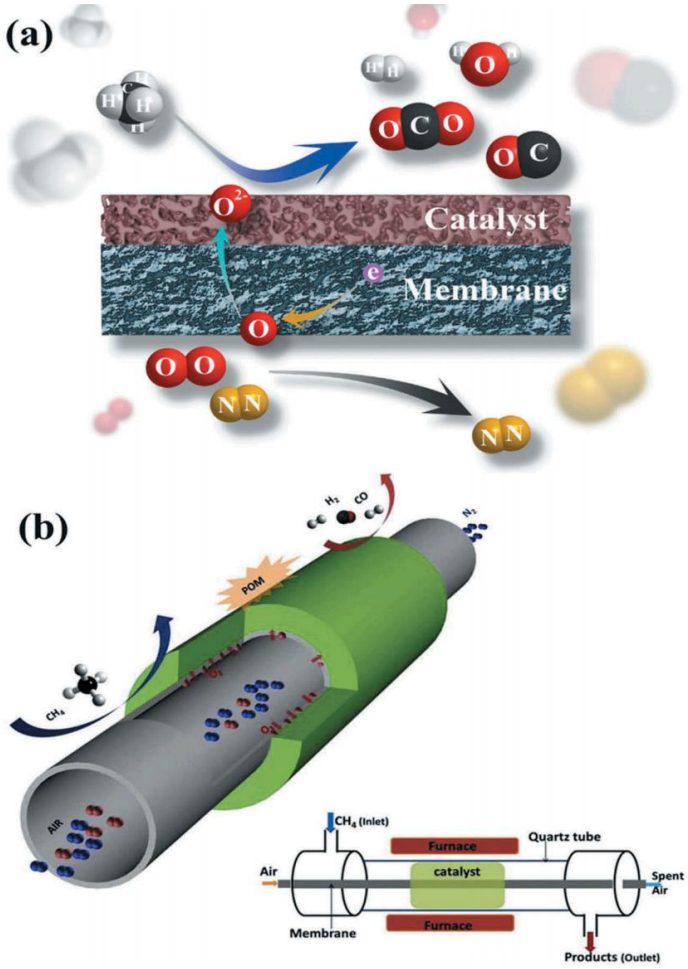

Figure 2-11 (a) Disk membrane reactor (b) Tabular membrane reactor [39]

POM in membrane reactor entails the following research activities:(1) Ensuring higher oxygen flow in the existence of reducing gases like CO, CH_4 and H_2 necessitates high-temperature membrane stability. (2) high CH_4 conversion and syngas ratio through altering membrane catalytic properties and surface adjustment (3) POM membrane designs that are novel. The next section discusses mixed ionic electronic membrane reactors with a catalyst layer that are disk-shaped.

2.5.3.1 Disk Membrane Reactors with Catalyst Layer

Membrane reactors with catalysts contain thin and porous catalyst layers over the inner side of the membrane as shown in Figure 2-11(a). The membrane reactor can

be a single or dual phase (composed of fluorite and perovskite) herein both are discussed.

The high oxygen separation capability of single-phase membranes makes it of immense interest to researchers. Different ceramic membranes with Ni-based catalysts have been investigated by different researchers for POM for example $BaCo_xFe_yZr_zO_{3-\delta}$ packed with Ni-based catalyst reported 96% methane conversion at 925 °C [67-69].

Ni-oxides supported over Al_2O_3 were intensively used with different membrane reactor for POM such as $Ba_{0.5}Sr_{0.5}Co_{0.8}Fe_{0.1}Ni_{0.1}O_{3-\delta}$ membrane reactor coated with Ni/Al_2O_3 reported 98% methane conversion at 850 °C [70], $BaCo_{0.4}Fe_{0.4}Zr_{0.2}O_{(3-\delta)}$ encrusted with $LiLaNiO/\gamma\text{-}Al_2O_3$ catalyst obtained 98% CH_4 conversion at 850 °C with 2 hour induction period [71], $SrCoFeO_x$ membrane reactor packed with $Ni/\gamma\text{-}Al_2O_3$ achieved CH_4 conversion of about 90% at 900 °C [72], $Ba_{0.15}Ce_{0.85}FeO_{(3-\delta)}$ layered with $LiLaNi/\gamma\text{-}Al_2O_3$ attained methane conversion of 96% at 850 °C at the cost of kinetic decomposition of material over membrane [73], $Sm_{0.2}Ce_{0.8}O_{2-\delta}$ (SDC)/γ–Al_2O_3 composite backed over Ni coated with $La_{0.6}Sr_{0.4}Co_{0.2}Fe_{0.8}O_{3-\delta}$ (LSCF) membrane produced 86% methane at a lesser temperature of 750 °C [74].

High temperature is yet required for high syngas production, despite the adoption of various membrane reactor configuration for POM. In most cases, membrane reactors can generate >90 percent syngas yield at high temperatures (850–950 °C) but increases energy consumption. As a result, extensive research is underway to develop membrane reactors which require low temperatures while sustaining syngas production.

Membrane reactors exhibiting high syngas production at 800 °C have recently been described in the literature. For example, Ni/ZrO_2 coated with $Ba_{0.5}Sr_{0.5}Co_{0.8}Fe_{0.2}O_{3-\delta}$ reported 80% methane conversion at 850 °C [75], $Sm_{0.2}Ce_{0.8}O_{2-\delta}$ (SDC)/γ–Al_2O_3 composite supported by Ni coated over $La_{0.6}Sr_{0.4}Co_{0.2}Fe_{0.8}O_{3-\delta}$ (LSCF) membrane produced 86% methane at lower temperature of 750 °C [74].

At a lower temperature, hollow-fiber membranes can generate high syngas output. For instance, a Ni/$LaAlO_3$-Al_2O_3 catalyst coated over hollow fibre membrane $La_{0.6}Sr_{0.4}Co_{0.8}Ga_{0.2}O_{3-\delta}$ reported 97% methane conversion at 750 °C [76] and $BaBi_{0.05}Co_{0.8}Nb_{0.15}O_{3-\delta}$ hollow fibre membrane integrated with Ni phyllosilicate catalyst achieved up to 80% methane conversion with stability of roughly 100 hours at a lower temperature of 730 °C.[66].

It's worth noting that developing membrane reactors that can work at lower temperature for POM faces two obstacles. :(i) POM is substantially affected by oxygen flux, it has a poor oxygen penetration rate at low temperatures, which inhibits methane conversion. As a result, obtaining high oxygen flux at temperatures below 800 °C is difficult, necessitating a reduction in methane flow rate and jeopardizing the system's potential for large-scale syngas production. (ii) The catalyst's limitations, since it produces syngas via a reforming mechanism that requires a greater temperature of over 800 °C for maximum syngas production. As a result, developing membrane materials and designs that offer high oxygen flux at low temperatures, as well as catalysts that produce syngas via direct partial oxidation, can make membrane reactors easier to operate. Some membrane reactors used in POM along with catalyst used, oxygen flux and methane conversion are summarized in Table 2-4.

Table 2-4 Membrane reactors utilized for POM

Membrane	Catalyst	T (°C)	XCH_4 (%)	Remarks	Ref
$La_{0.6}Sr_{0.4}Co_{0.2}Fe_{0.8}O_{3-\delta}$	$Sm_{0.2}Ce_{0.8}O_{2-\delta}$ (SDC)/γ–Al_2O_3 supported Ni	750	86	Oxygen vacancies introduced into the catalytic layer increased methane DPO and preserves active oxygen species in catalysis	[74]
$BaBi_{0.05}Co_{0.8}Nb_{0.15}O_{3-\delta}$	Ni	750	80	High hydrogen production yields are enabled by the optimal ratio of oxygen permeation flow to methane feeding rate.	[66]
$BaCo_xFe_yZr_zO_{3-\delta}$	Ni	925	96	To ensure complete reforming reaction catalyst should be packed at the back of hollow fibre membrane	[67]
$BaCo_{0.7}Fe_{0.2}Nb_{0.1}O_{3-\delta}$	Ni	875	92	The BCFNO membrane was discovered to have poor catalytic activity for the oxidation of CH4 in COG.	[69]
$BaCo_{0.4}Fe_{0.4}Zr_{0.2}O_{3-\delta}$	LiLaNiO/γ-Al_2O_3	850	96–98	BCFZO, a novel zirconium-based perovskite material shows high structural stability, long-term stability, and oxygen penetration flux.	[71]
$SrCoFeO_x$	Ni/γ-Al_2O_3	900	90	The activity for oxidation of the reducing gas enhances the oxygen penetration flux across a mixed-conducting ceramic membrane with a reducing gas as the sweep gas.	[72]
$La_{0.6}Sr_{0.4}Co_{0.2}Fe_{0.8}O_{3-\delta}$	Ni/γ-Al_2O_3	885	96	For partial oxidation of methane to syngas, NiO/-Al_2O_3 may not be appropriate for use in the membrane reactor.	[28]

2.6 Catalyst System for POM

Ni supported POM was first investigated by Prettre et al. in which they reported that syngas is produced through burning of methane followed by CO_2 and H_2O reforming. Since 1990 POM has caught the attention of the researcher around the world with initial focus on catalyst screening, reaction conditions, catalyst stability and catalytic activity. Until various catalyst system such as noble metals, transitional metals and different perovskite are investigated for POM. The Ni based catalyst system are the most used catalyst system for POM owing to it low price, abundance, and high catalytic activity at lower temperature [77].

2.6.1 Nickel Based Catalyst System for POM

Nickel based catalyst system are good alternative to the expensive and rare noble metals. Nickel based catalyst have reposted >96 % methane conversion and >96% syngas selectivity making it it competitive to the noble metals however it has a problem of carbon deposition that deactivate the catalysts in the long run. Other issues that affect the Ni-based catalyst performance is the depletion of active metal sites, sintering, and change in the catalyst structure due to hotspot formation. Therefor researchers are focusing on to improve Ni-based catalyst system through different techniques such as improving synthesis methods, support modification and adding different promoters.

This section describes the impact of promoter and support over the catalytic activity of Ni-based catalysts. Various supports systems for instance BaO, MgO, SrO, CaO, Sm_2O_3, Yb_2O_3 and La_2O_3 are investigated in the literature to alter the Ni-based catalyst properties to get the desired catalytic activity [78, 79]. MgO at 800 °C had good catalytic activity with 95 % CH_4 conversion, 95 % H_2 selectivity and 97.5 % CO selectivity [79]. The interaction of Ni-NiOx with Al_2O_3-$NiAl_2O_4$ nanofibrous support, on the other hand, has been shown to minimize Ni aggregation with catalytic activity of 98.5 % CH_4 conversion, 97.4 % H_2 selectivity and 98.5 % CO selectivity at 850 °C [80].

High catalytic activity for POM at 500 and 600 °C is shown by Ni/Al_2O_3/MgO and Ni/sorbacid catalysts. High basicity favors the WGSR and the reverse Boudouard

reaction [81]. Furthermore, Ni/TiO2 catalytic activity in POM and DRM has been documented With 88.2 percent CO and 99.7 percent H_2 selectivity, 86.3 percent CH_4 conversion was achieved [82].

Tuning support acidity is another technique to change catalyst surface and metal-support interaction [83]. SiO_2-Al_2O_3, SiO_2-ZrO_2 and H-Y Zeolite supports have been investigated. The results obtained from Ni loading of 5% supported with SiO_2-ZrO_2 were 96.1% CH_4 conversion, 99.4 % H_2 selectivity and 97.2 % CO selectivity. H-Y zeolite reported the lowest catalytic performance. Silica-zirconia exhibited for excellent conversion of CH_4 and syngas selectivity due to it lower acidity, but zeolites have a high acidity, which reduces its catalytic performance. The 25% CeO_2-ZrO_2 integrated with ZSM-5 helped Ni lower the POM temperature of equilibrium. Furthermore, at 700 °C, CH_4 conversion of up to 90% was accomplished [84]

POM was performed on an aluminosilicate support with several active metals such as Fe, Cr, Ni, Co and Cu 45 [85]. At 800 degrees Celsius, Ni supported produced 93 % CH_4 conversion, 95 % H_2 selectivity and 94 % CO selectivity. However, the creation of CO_2 was favored by Co, Fe, Cr, and Cu, with no appreciable syngas production. At 450–750°C and 1atm, Berrocal et al. examined Ni catalysts supported over zirconia-alumina support with Al/Zr ratio of 2 at 750 °C produced up to 82 % H_2 selectivity and 85 % CH_4 conversion [86]. Besides zeolites, the effect of calcination temperature and acidity on Ni/Y_2O_3 catalysts is well documented [87]. Low calcination temperature has been linked to decreased acidity and lower Ni/Y_2O_3 interaction. The active sites migrate and clump together due to the low acidity of support, this results in the decline from 84% to 77% CH_4 conversion.

The basicity and acidity of Support affects the POM. High support basicity reduces carbon deposition though carbon species oxidation. Ozmedir et al. stated that decreasing basicity of Ni/Al_2O_3 catalyst by doping it with Mg increased the carbon deposition rate. The oxidation of carbon species over catalyst surface by reverse Boudouard reaction, is aided by support basicity [81]. Similarly, using a Ni/ZrO2 catalyst with high concentration of Lewis basic acid sites promotes CO_2 adsorption and conversion to CO [88]. The H_2/CO ratio is reduce by the reverse Boudouard reaction.

The catalyst activity along with the acidic or basic nature, are influenced by support reducibility.CO disproportionation over catalyst surface is determined by the reducibility of the support. This reaction can result in the increased production of CO_2 and a decrease in syngas selectivity. The reduction of support and the breakdown of CH_4 over Ni/CaO, Ni/CeO_2 and Ni/MgO was investigated by Tang et al. In comparison to Ni/CeO_2 and Ni/CaO, the Ni/MgO demonstrated stronger resistance to CO disproportionation for 100 hours due to its low reducibility [89]. Because of its great reducibility,

In the literature CeO_2 as a Ni catalyst support is investigated extrensively. By the utilization of microwave-assisted co-precipitation, hydrothermal, and impregnation procedures for synthesis, Pantaleo et al. found outstanding performance of Ni/CeO_2 At 800 °C, methane conversion was 98 % with 95 % CO selectivity which is credited to reduction by CeO_2 and CH_4 dissociation over catalyst surface, that favor CO production rather than carbon deposition. It's worth noting that Ce boosted mobility of oxygen, which resulted in more CO production. Pantaleo et al. also observed that replacing the Ni/CeO_2 catalyst support with La_2O_3 resulted in a lower catalytic activity temperature, which was validated by TPR experiments due to reduced reducibility [90]. Singha et al. also found outstanding POM performance from nanoscale Ni-CeO_2. According on TPR study, the nano-scaled catalyst had a high reducibility and accomplished 98 % CH_4 conversion and 95 % > syngas selectivity. Due to the minimal amount of carbon deposition, the catalyst remained stable over a 100-hour period of operation, with a slight drop in con- version [91]. Peyman et al. documented a CeO_2 supported Ni catalyst with a high surface area that obtained up to 90% CH_4 conversion and 90% CO selectivity [92]. In addition to reducing catalysts, CeO_2 has been proven to promote Ni dispersion, resulting in increased syngas production over Ni/CeO_2- SiO_2 catalysts [93].

The influence of promoters on Ni-based catalysts has been well documented; they have been shown to improve Ni-based catalytic performance by reducing ignition temperature and minimizing carbon deposition. The ignition temperature of NiO_x/Al_2O_3 has been reported to be reduced by noble metals and metal oxides [79, 94]. The ignition temperature was dropped to 530 °C when Pt was added to Ni/Al_2O_3. At 900 °C, a $Ni/Li/La_2O_3/Al_2O_3$ catalyst was reported to be stable during a 200-hour

POM reaction, with 96 % methane conversion. When NiO/Al_2O_3 was promoted with La_2O_3, the ignition temperature of NiO/Al2O3 was lowered, according to the literature. Carbon deposition on a NiO/Al_2O_3 catalyst was found to be decreased by La_2O_3, whereas CaO addition entirely inhibited carbon deposition [94-96].

Promoters are also important for improving reducibility. The addition of Na, Sr, Ce, and La to the support, for example, has been shown to improve Ni/Al_2O_3 reducibility. Due to the absence of substantial metal-support interaction, Ce addition resulted in a 92 % CH_4 conversion. [15] As a result, Ce addition has the effect of lowering catalyst reduction temperature. [37] Ferreira et al. investigated the influence of Gd, Lu, and Pr as promoters on the synergetic effect of La_2O_3 on NiO catalyst. At 750 °C, syngas selectivity reached up to 80% while CH_4 conversion approached 90%. [97]The action of La_2O_3 on $Ni/Ce-ZrO_2$ has been seen in a similar way[98]

By combining promoters with appropriate support, such as Y_2O_3, ZrO_2, Al_2O_3, MgO, SiO_2, and TiO_2 the catalytic activity can be improved. The addition of Cu and Fe to the $(Ni_xMg_{1-x})Al_y$ catalyst was investigated. The addition of Cu increased selectivity to CO and H_2 by 53 and 41 percent, respectively. The inclusion of Fe, on the other hand, enhanced complete combustion and water-gas shift processes. Reducibility of Cu-Ni-Mg/Al catalysts has also been found due to the Cu effect [99]. Rh-promoted Ni catalysts have also been tested on a variety of supports, including Al_2O_3, MgO, CeO_2, ZrO_2, and La_2O_3. It has been claimed that adding Rh promoter increased Ni reduction and carbon deposition, resulting in up to 90% syngas selectivity and 90% CH_4 conversion at 750°C [88]. Furthermore, due to carbon deposition resistance, the activity of the Ni/Al2O3 catalyst in POM was increased by the addition of Re (100 CH_4 conversion was accomplished) [100].In the Ni/ZrO_2 system, less common promoters like PrO_2 have been impregnated. Due to substantial metal dispersion and metal-support interaction, the data revealed that PrO_2 contributed to the creation of NiO active phases.

In terms of CH_4 conversion and syngas selectivity, Ni-based catalysts are more active than Co-based catalysts. However, to reduce carbon emissions, their stability must be improved. Recent investigations have shown that, in addition to promoter doping and selecting appropriate support, modifying catalyst structure can reduce

carbon deposition since carbon deposition is structural-sensitive to Ni catalyst [101, 102]

2.6.2 Biomass Fly Ash as Catalyst Support

The power plants that use solid fuels such as coal and biomass as fuel produce large amounts of both bottom ash and fly ash, and its management and disposal are a major concern for the global environmental crisis. Typically, these ashes are disposed of in landfills. However, various academics from all over the world are now interested in long-term waste ash management in order to maximize waste material recovery Coal fly ash has been successfully used in road construction, cement manufacture, building materials such as concrete, and zeolite preparation, according to the literature.[103].

Coal ash contains a variety of metal oxides, including Al_2O_3, Fe_2O_3, SiO_2, and MgO [28], making it a good choice for catalytic use. Another study employed a Ni-based catalyst backed by coal ash for steam reforming of acetic acid and phenol to produce hydrogen. The results showed that in the presence of a coal ash supported catalyst, hydrogen generation and reactant conversion were greatly increased [104]. To produce hydrogen and syngas, steam gasification of palm shell was investigated using coal ash as a catalyst. The yield of hydrogen and syngas is affected by the presence of coal ash [105]. In the biomass steam reforming process for the production of hydrogen, ash obtained from the combustion of various solid fuels and waste, such as coal, waste rubber tyres, and refuse-derived carbon, was also used as a catalyst's support, with promising results because the metal oxide present in the catalyst's support (ashes) aided in catalytic activity [106].

Assad et al. researched into the handling and long-term management of biomass fly ash (BFA), which is produced by biomass-fired power plants. The author used a variety of characterisation approaches to quickly determine the various physiochemical properties of BFA. Because it comprises diverse metal oxides such as Al_2O_3, Fe_2O_3, SiO_2, MgO, $CaCO_3$, and K_2O and has a flake-like shape, the findings show that BFA could be utilised for catalysis, among other things. Despite their favourable physiochemical features, BFA has been persistently overlooked for catalytic applications in the literature.

Summary

Excessive use of fossil fuel resources to meet global energy demand depletes fossil fuel supplies and increases GHG concentrations in our environment. Researchers from all over the world are working on both challenges at the same time. Renewable energy adoption and development are some of the solutions to the problems at hand, however, these technologies are still immature and inefficient. As a result, efficient fossil fuel utilization is required to address both fossil fuel depletion and GHG emissions. Partial oxidation of methane (POM), dry reforming of methane (DRM), steam reforming of methane (SRM), and coal gasification are some of the technologies used to convert methane to hydrogen. The commercial hydrogen production processes include DRM and POM. Hydrogen generation systems based on renewable energy include thermochemical water splitting, photo-electrolysis, electrolysis, and biomass gasification. These procedures are in high demand due to their use of renewable energy and sources; however, these are in the developmental stages. Aside from that, POM is another way to generate hydrogen gas.

The diverse ashes produced by power plants are often dumped in landfill locations, resulting in total bio-material waste. The physiochemical properties of these ashes were thoroughly investigated in the literature for sustainable management, and the presence of various oxides made it a promising candidate for catalytic applications.

The primary issue with partial methane oxidation is the premature deactivation of the catalysts caused by the formation of hot spots. Different catalysts have been used to solve this problem, but no significant progress has been made. To address the costs of the catalyst for POM, sustainable materials were sought for use in POM.

Various reactor systems were utilized in the POM to increase hydrogen generation while avoiding catalyst deactivation owing to deposition of carbon. Fixed bed reactors were mostly used because they are easy to handle and provide maximum heat transfer to the catalytic bed, which improves methane conversion and hydrogen generation.

References

[1] A.P.E. York, T. Xiao, M.L.H. Green, Brief Overview of the Partial Oxidation of Methane to Synthesis Gas, Topics in Catalysis, 22 (2003) 345-358.

[2] J.H. Lunsford, Catalytic conversion of methane to more useful chemicals and fuels: a challenge for the 21st century, Catalysis Today, 63 (2000) 165-174.

[3] M. Soltanieh, A. Zohrabian, M.J. Gholipour, E. Kalnay, A review of global gas flaring and venting and impact on the environment: Case study of Iran, International Journal of Greenhouse Gas Control, 49 (2016) 488-509.

[4] N.J. Themelis, P.A. Ulloa, Methane generation in landfills, Renewable Energy, 32 (2007) 1243-1257.

[5] M.N. Dunkle, W.L. Winniford. Catalysis Today, 63 (2000) 165-174.

[6] M.C.J. Bradford, M.A. Vannice, CO_2 Reforming of CH_4 over Supported Ru Catalysts, Journal of Catalysis, 183 (1999) 69-75.

[7] J.B. Claridge, A.P.E. York, A.J. Brungs, C. Marquez-Alvarez, J. Sloan, S.C. Tsang, M.L.H. Green, New Catalysts for the Conversion of Methane to Synthesis Gas: Molybdenum and Tungsten Carbide, Journal of Catalysis, 180 (1998) 85-100.

[8] A. Theampetch, C. Prapainainar, S. Tungkamani, P. Narataruksa, T. Sornchamni, L. Árnadóttir, G.N. Jovanovic, Detailed microkinetic modelling of syngas to hydrocarbons via Fischer Tropsch synthesis over cobalt catalyst, International Journal of Hydrogen Energy, (2020).

[9] R.B. Anderson, Fischer-Tropsch synthesis, Academic Press,London, England, United Kingdom, 1984.

[10] A. Abdulrasheed, A.A. Jalil, Y. Gambo, M. Ibrahim, H.U. Hambali, M.Y. Shahul Hamid, A review on catalyst development for dry reforming of methane to syngas: Recent advances, Renewable and Sustainable Energy Reviews, 108 (2019) 175-193.

[11] K. de Oliveira Rocha, C.M.P. Marques, J.M.C. Bueno, Effect of Au doping of Ni/Al_2O_3 catalysts used in steam reforming of methane: Mechanism, apparent activation energy, and compensation effect, Chemical Engineering Science, 207 (2019) 844-852.

[12] A. Emamdoust, V. La Parola, G. Pantaleo, M.L. Testa, S. Farjami Shayesteh, A.M. Venezia, Partial oxidation of methane over SiO_2 supported Ni and NiCe catalysts, Journal of Energy Chemistry, 47 (2020) 1-9.

[13] Sharma, Poelman, Marin, Galvita, Approaches for Selective Oxidation of Methane to Methanol, Catalysts, 10 (2020) 194.

[14] P.O. Sharma, M.A. Abraham, S. Chattopadhyay, Development of a Novel Metal Monolith Catalyst for Natural Gas Steam Reforming, Industrial & Engineering Chemistry Research, 46 (2007) 9053-9060.

[15] V.H. Collins-Martinez, J.F. Cazares-Marroquin, J.M. Salinas-Gutierrez, J.C. Pantoja-Espinoza, A. Lopez-Ortiz, M.J. Melendez-Zaragoza, The thermodynamic evaluation and

process simulation of the chemical looping steam methane reforming of mixed iron oxides, RSC Advances, 11 (2021) 684-699.

[16] E. Meloni, M. Martino, V. Palma, A Short Review on Ni Based Catalysts and Related Engineering Issues for Methane Steam Reforming, Catalysts, 10 (2020) 352.

[17] R. Carapellucci, L. Giordano, Steam, dry and autothermal methane reforming for hydrogen production: A thermodynamic equilibrium analysis, Journal of Power Sources, 469 (2020) 228391.

[18] C. Shi, S. Wang, X. Ge, S. Deng, B. Chen, J. Shen, A review of different catalytic systems for dry reforming of methane: Conventional catalysis-alone and plasma-catalytic system, Journal of CO2 Utilization, 46 (2021) 101462.

[19] H. Zhang, Y. Shuai, S. Pang, R. Pan, B.G. Lougou, X. Huang, Numerical Investigation of Carbon Deposition Behavior in Ni/Al_2O_3-Based Catalyst Porous-Filled Solar Thermochemical Reactor for the Dry Reforming of Methane Process, Industrial & Engineering Chemistry Research, 58 (2019) 15701-15711.

[20] T. Stroud, T.J. Smith, E. Le Saché, J.L. Santos, M.A. Centeno, H. Arellano-Garcia, J.A. Odriozola, T.R. Reina, Chemical CO_2 recycling via dry and bi reforming of methane using Ni-Sn/Al_2O_3 and Ni-Sn/CeO_2-Al_2O_3 catalysts, Applied Catalysis B: Environmental, 224 (2018) 125-135.

[21] S. Singh, M.B. Bahari, B. Abdullah, P.T.T. Phuong, Q.D. Truong, D.-V.N. Vo, A.A. Adesina, Bi-reforming of methane on Ni/SBA-15 catalyst for syngas production: Influence of feed composition, International Journal of Hydrogen Energy, 43 (2018) 17230-17243.

[22] D.B.L. Santos, F.B. Noronha, C.E. Hori, Bi-reforming of methane for hydrogen production using $LaNiO_3/CexZr_{1-x}O_2$ as precursor material, International Journal of Hydrogen Energy, 45 (2020) 13947-13959.

[23] B. Tahir, M. Tahir, N.A.S. Amin, Silver loaded protonated graphitic carbon nitride (Ag/pg-C_3N_4) nanosheets for stimulating CO_2 reduction to fuels via photocatalytic bi-reforming of methane, Applied Surface Science, 493 (2019) 18-31.

[24] D. He, Y. Zhang, Z. Wang, Y. Mei, Y. Jiang, Bi-reforming of Methane with Carbon Dioxide and Steam on Nickel-Supported Binary Mg–Al Metal Oxide Catalysts, Energy & Fuels, 34 (2020) 4822-4827.

[25] S. Kim, B.S. Crandall, M.J. Lance, N. Cordonnier, J. Lauterbach, E. Sasmaz, Activity and stability of NiCe@SiO_2 multi–yolk–shell nanotube catalyst for tri-reforming of methane, Applied Catalysis B: Environmental, 259 (2019) 118037.

[26] E. Rezaei, L.J.J. Catalan, Evaluation of CO_2 utilization for methanol production via tri-reforming of methane, Journal of CO2 Utilization, 42 (2020) 101272.

[27] R. Kumar, K. Kumar, N.V. Choudary, K.K. Pant, Effect of support materials on the performance of Ni-based catalysts in tri-reforming of methane, Fuel Processing Technology, 186 (2019) 40-52.

[28] R. Jin, Y. Chen, W. Li, W. Cui, Y. Ji, C. Yu, Y. Jiang, Mechanism for catalytic partial oxidation of methane to syngas over a Ni/Al_2O_3 catalyst, Applied Catalysis A: General, 201 (2000) 71-80.

[29] N. Hadian, M. Rezaei, Combination of dry reforming and partial oxidation of methane over Ni catalysts supported on nanocrystalline $MgAl_2O_4$, Fuel, 113 (2013) 571-579.

[30] Q. Duan, J. Wang, C. Ding, H. Ding, S. Guo, Y. Jia, P. Liu, K. Zhang, Partial oxidation of methane over Ni based catalyst derived from order mesoporous $LaNiO_3$ perovskite prepared by modified nanocasting method, Fuel, 193 (2017) 112-118.

[31] A.H. Khoja, M. Tahir, N.A. Saidina Amin, Evaluating the Performance of a Ni Catalyst Supported on La_2O_3-$MgAl_2O_4$ for Dry Reforming of Methane in a Packed Bed Dielectric Barrier Discharge Plasma Reactor, Energy & Fuels, 33 (2019) 11630-11647.

[32] B. Li, H. Li, W.-Z. Weng, Q. Zhang, C.-J. Huang, H.-L. Wan, Synthesis gas production from partial oxidation of methane over highly dispersed Pd/SiO_2 catalyst, Fuel, 103 (2013) 1032-1038.

[33] J.A. Velasco, C. Fernandez, L. Lopez, S. Cabrera, M. Boutonnet, S. Järås, Catalytic partial oxidation of methane over nickel and ruthenium based catalysts under low O_2/CH_4 ratios and with addition of steam, Fuel, 153 (2015) 192-201.

[34] Y. Ma, Y. Ma, Y. Chen, S. Ma, Q. Li, X. Hu, Z. Wang, C.E. Buckley, D. Dong, Highly stable nanofibrous La_2NiZrO_6 catalysts for fast methane partial oxidation, Fuel, 265 (2020) 116861.

[35] Q. Shen, F. Huang, M. Tian, Y. Zhu, L. Li, J. Wang, X. Wang, Effect of Regeneration Period on the Selectivity of Synthesis Gas of Ba-Hexaaluminates in Chemical Looping Partial Oxidation of Methane, ACS Catalysis, 9 (2019) 722-731.

[36] S. Chen, L. Zeng, H. Tian, X. Li, J. Gong, Enhanced Lattice Oxygen Reactivity over Ni-Modified WO_3-Based Redox Catalysts for Chemical Looping Partial Oxidation of Methane, ACS Catalysis, 7 (2017) 3548-3559.

[37] S. Bhavsar, G. Veser, Chemical looping beyond combustion: production of synthesis gas via chemical looping partial oxidation of methane, RSC Advances, 4 (2014) 47254-47267.

[38] J. Zhang, T. He, Z. Wang, M. Zhu, K. Zhang, B. Li, J. Wu, The search of proper oxygen carriers for chemical looping partial oxidation of carbon, Applied Energy, 190 (2017) 1119-1125.

[39] A.H. Elbadawi, L. Ge, Z. Li, S. Liu, S. Wang, Z. Zhu, Catalytic partial oxidation of methane to syngas: review of perovskite catalysts and membrane reactors, Catalysis Reviews, (2020) 1-67.

[40] J.H. Kim, Y.S. Jang, J.C. Kim, D.H. Kim, Anodic aluminum oxide supported Cu-Zn catalyst for oxidative steam reforming of methanol, Korean Journal of Chemical Engineering, 36 (2019) 368-376.

[41] Y. Ji, W. Li, H. Xu, Y. Chen, Catalytic partial oxidation of methane to synthesis gas over Ni/γ-Al_2O_3 catalyst in a fluidized-bed, Applied Catalysis A: General, 213 (2001) 25-31.

[42] T. Ostrowski, A. Giroir-Fendler, C. Mirodatos, L. Mleczko, Comparative study of the catalytic partial oxidation of methane to synthesis gas in fixed-bed and fluidized-bed membrane reactors: Part I: A modeling approach, Catalysis Today, 40 (1998) 181-190.

[43] J. Kim, Y. Ryou, T.H. Kim, G. Hwang, J. Bang, J. Jung, Y. Bang, D.H. Kim, Highly selective production of syngas (>99%) in the partial oxidation of methane at 480 °C over Pd/CeO2 catalyst promoted by HCl, Applied Surface Science, 560 (2021) 150043.

[44] L. Ma, C. Ding, J. Wang, Y. Li, Y. Xue, J. Guo, K. Zhang, P. Liu, X. Gao, Highly dispersed Pt nanoparticles confined within hierarchical pores of silicalite-1 zeolite via crystal transformation of supported Pt/S-1 catalyst for partial oxidation of methane to syngas, International Journal of Hydrogen Energy, 44 (2019) 21847-21857.

[45] R. Chai, Z. Zhang, P. Chen, G. Zhao, Y. Liu, Y. Lu, Ni-foam-structured NiO-MOx-Al_2O_3 (M = Ce or Mg) nanocomposite catalyst for high throughput catalytic partial oxidation of methane to syngas, Microporous and Mesoporous Materials, 253 (2017) 123-128.

[46] R. Jalali, M. Rezaei, B. Nematollahi, M. Baghalha, Preparation of Ni/$MeAl_2O_4$-$MgAl_2O_4$ (Me=Fe, Co, Ni, Cu, Zn, Mg) nanocatalysts for the syngas production via combined dry reforming and partial oxidation of methane, Renewable Energy, 149 (2020) 1053-1067.

[47] A. Khaleel, S. Jobe, M.a. Ahmed, S. Al-Zuhair, S. Tariq, Enhanced selectivity of syngas in partial oxidation of methane: A new route for promising Ni-alumina catalysts derived from Ni/γ-AlOOH with modified Ni dispersion, International Journal of Energy Research, 44 (2020) 12081-12099.

[48] A. Moral, I. Reyero, J. Llorca, F. Bimbela, L.M. Gandía, Partial oxidation of methane to syngas using Co/Mg and Co/Mg-Al oxide supported catalysts, Catalysis Today, 333 (2019) 259-267.

[49] J. Wang, L. Ma, C. Ding, Y. Xue, Y. Zhang, Z. Gao, In Situ Encapsulated Pt Nanoparticles Dispersed in Low Temperature Oxygen for Partial Oxidation of Methane to Syngas, Catalysts, 9 (2019) 720.

[50] S. Guo, J. Wang, C. Ding, Q. Duan, Q. Ma, K. Zhang, P. Liu, Confining Ni nanoparticles in honeycomb-like silica for coking and sintering resistant partial oxidation of methane, International Journal of Hydrogen Energy, 43 (2018) 6603-6613.

[51] S. Somacescu, N. Cioatera, P. Osiceanu, J.M. Calderon-Moreno, C. Ghica, F. Neaţu, M. Florea, Bimodal mesoporous NiO/CeO_2-δ-YSZ with enhanced carbon tolerance in catalytic partial oxidation of methane—Potential IT-SOFCs anode, Applied Catalysis B: Environmental, 241 (2019) 393-406.

[52] J.C.S. Araújo, L.F. Oton, A.C. Oliveira, R. Lang, L. Otubo, J.M.C. Bueno, On the role of size controlled Pt particles in nanostructured Pt-containing Al_2O_3 catalysts for partial oxidation of methane, International Journal of Hydrogen Energy, 44 (2019) 27329-27342.

[53] A. Mosayebi, Kinetic modeling of catalytic partial oxidation of methane over Ni-Rh/γ-Al_2O_3 catalyst for syngas formation, Journal of the Taiwan Institute of Chemical Engineers, 114 (2020) 36-46.

[54] S.V. Dhodapkar, A. Zaltash, G. Klinzing, A primer on gas-solids fluidization, 119 (2012) 38-47.

[55] U. Olsbye, E. Tangstad, I.M. Dahl, Partial oxidation of methane to synthesis gas in a fluidized bed reactor, in: H.E. Curry-Hyde, R.F. Howe (Eds.) Studies in Surface Science and Catalysis, Elsevier1994, pp. 303-308.

[56] Y. Matsuo, Y. Yoshinaga, Y. Sekine, K. Tomishige, K. Fujimoto, Autothermal CO_2 reforming of methane over NiO–MgO solid solution catalysts under pressurized condition: Effect of fluidized bed reactor and its promoting mechanism, Catalysis Today, 63 (2000) 439-445.

[57] L. Mo, X. Zheng, Q. Jing, H. Lou, J. Fei, Combined Carbon Dioxide Reforming and Partial Oxidation of Methane to Syngas over Ni−La_2O_3/SiO_2 Catalysts in a Fluidized-Bed Reactor, Energy & Fuels, 19 (2005) 49-53.

[58] A. Santos, M. Menéndez, J. Santaríana, Partial oxidation of methane to carbon monoxide and hydrogen in a fluidized bed reactor, Catalysis Today, 21 (1994) 481-488.

[59] Q. Jing, H. Lou, L. Mo, J. Fei, X. Zheng, Combination of CO_2 reforming and partial oxidation of methane over Ni/BaO-SiO_2 catalysts to produce low H_2/CO ratio syngas using a fluidized bed reactor, Journal of Molecular Catalysis A: Chemical, 212 (2004) 211-217.

[60] L. Mleczko, T. Wurzel, Experimental studies of catalytic partial oxidation of methane to synthesis gas in a bubbling-bed reactor, Chemical Engineering Journal, 66 (1997) 193-200.

[61] K.-J. Marschall, L. Mleczko, Experimental Investigations of Catalytic Partial Oxidation of Methane to Synthesis Gas in Various Types of Fluidized-Bed Reactors, Chemical Engineering & Technology, 23 (2000) 31-37.

[62] S. Bhatia, C.Y. Thien, A.R. Mohamed, Oxidative coupling of methane (OCM) in a catalytic membrane reactor and comparison of its performance with other catalytic reactors, Chemical Engineering Journal, 148 (2009) 525-532.

[63] J. Caro, H.H. Wang, C. Tablet, A. Kleinert, A. Feldhoff, T. Schiestel, M. Kilgus, P. Kölsch, S. Werth, Evaluation of perovskites in hollow fibre and disk geometry in catalytic membrane reactors and in oxygen separators, Catalysis Today, 118 (2006) 128-135.

[64] J. Sunarso, S. Baumann, J.M. Serra, W.A. Meulenberg, S. Liu, Y.S. Lin, J.C. Diniz da Costa, Mixed ionic–electronic conducting (MIEC) ceramic-based membranes for oxygen separation, Journal of Membrane Science, 320 (2008) 13-41.

[65] Z. Wang, Z. Li, Y. Cui, T. Chen, J. Hu, S. Kawi, Highly Efficient NO Decomposition via Dual-Functional Catalytic Perovskite Hollow Fiber Membrane Reactor Coupled with Partial Oxidation of Methane at Medium-Low Temperature, Environmental Science & Technology, 53 (2019) 9937-9946.

[66] Z. Wang, J. Ashok, Z. Pu, S. Kawi, Low temperature partial oxidation of methane via $BaBi_{0.05}Co_{0.8}Nb_{0.15}O_{3-\delta}$-Ni phyllosilicate catalytic hollow fiber membrane reactor, Chemical Engineering Journal, 315 (2017) 315-323.

[67] H. Wang, C. Tablet, T. Schiestel, S. Werth, J. Caro, Partial oxidation of methane to syngas in a perovskite hollow fiber membrane reactor, Catalysis Communications, 7 (2006) 907-912.

[68] H. Wang, A. Feldhoff, J. Caro, T. Schiestel, S. Werth, Oxygen selective ceramic hollow fiber membranes for partial oxidation of methane, AIChE Journal, 55 (2009) 2657-2664.

[69] Y. Zhang, J. Liu, W. Ding, X. Lu, Performance of an oxygen-permeable membrane reactor for partial oxidation of methane in coke oven gas to syngas, Fuel, 90 (2011) 324-330.

[70] E.G. Babakhani, J. Towfighi, Z. Taheri, A.N. Pour, M. Zekordi, A. Taheri, Partial oxidation of methane in $Ba_{0.5}Sr_{0.5}Co_{0.8}Fe_{0.1}Ni_{0.1}O_{3-\delta}$ ceramic membrane reactor, Journal of Natural Gas Chemistry, 21 (2012) 519-525.

[71] J. Tong, W. Yang, R. Cai, B. Zhu, L. Lin, Novel and Ideal Zirconium-Based Dense Membrane Reactors for Partial Oxidation of Methane to Syngas, Catalysis Letters, 78 (2002) 129-137.

[72] J. Kniep, Y.S. Lin, Partial Oxidation of Methane and Oxygen Permeation in SrCoFeOx Membrane Reactor with Different Catalysts, Industrial & Engineering Chemistry Research, 50 (2011) 7941-7948.

[73] X. Zhu, H. Wang, Y. Cong, W. Yang, Partial oxidation of methane to syngas in $BaCe_{0.15}Fe_{0.85}O_{3-\delta}$ membrane reactors, Catalysis Letters, 111 (2006) 179-185.

[74] A.H. Elbadawi, L. Ge, J. Zhang, L. Zhuang, S. Liu, X. Tan, S. Wang, Z. Zhu, Partial oxidation of methane to syngas in catalytic membrane reactor: Role of catalyst oxygen vacancies, Chemical Engineering Journal, 392 (2020) 123739.

[75] Z. Shen, P. Lu, J. Hu, X. Hu, Performance of $Ba_{0.5}Sr_{0.5}Co_{0.8}Fe_{0.2}O_{3+\delta}$ membrane after laser ablation for methane conversion, Catalysis Communications, 11 (2010) 892-895.

[76] Y. Kathiraser, S. Kawi, $La_{0.6}Sr_{0.4}Co_{0.8}Ga_{0.2}O_{3-\delta}$ (LSCG) hollow fiber membrane reactor: Partial oxidation of methane at medium temperature, AIChE Journal, 59 (2013) 3874-3885.

[77] N.S.N. Hasnan, S.N. Timmiati, K.L. Lim, Z. Yaakob, N.H.N. Kamaruddin, L.P. Teh, Recent developments in methane decomposition over heterogeneous catalysts: an overview, Materials for Renewable and Sustainable Energy, 9 (2020) 8.

[78] V.R. Choudhary, A.M. Rajput, B. Prabhakar, A.S. Mamman, Partial oxidation of methane to CO and H_2 over nickel and/or cobalt containing ZrO_2, ThO_2, UO_2, TiO_2 and SiO_2 catalysts, Fuel, 77 (1998) 1803-1807.

[79] V.R. Choudhary, B.S. Uphade, A.S. Mamman, Large enhancement in methane-to-syngas conversion activity of supported Ni catalysts due to precoating of catalyst supports with MgO, CaO or rare-earth oxide, Catalysis Letters, 32 (1995) 387-390.

[80] Z. Wang, Y. Cheng, X. Shao, J.-P. Veder, X. Hu, Y. Ma, J. Wang, K. Xie, D. Dong, S. Ping Jiang, G. Parkinson, C. Buckley, C.-Z. Li, Nanocatalysts anchored on nanofiber support for high syngas production via methane partial oxidation, Applied Catalysis A: General, 565 (2018) 119-126.

[81] H. Özdemir, M.A. Faruk Öksüzömer, M. Ali Gürkaynak, Preparation and characterization of Ni based catalysts for the catalytic partial oxidation of methane: Effect of support basicity on H_2/CO ratio and carbon deposition, International Journal of Hydrogen Energy, 35 (2010) 12147-12160.

[82] Q.G. Yan, W.Z. Weng, H.L. Wan, H. Toghiani, R.K. Toghiani, C.U. Pittman, Activation of methane to syngas over a Ni/TiO_2 catalyst, Applied Catalysis A: General, 239 (2003) 43-58.

[83] W.J.M. Vermeiren, E. Blomsma, P.A. Jacobs, Catalytic and thermodynamic approach of the oxyreforming reaction of methane, Catalysis Today, 13 (1992) 427-436.

[84] A.I. Osman, J. Meudal, F. Laffir, J. Thompson, D. Rooney, Enhanced catalytic activity of Ni on η-Al_2O_3 and ZSM-5 on addition of ceria zirconia for the partial oxidation of methane, Applied Catalysis B: Environmental, 212 (2017) 68-79.

[85] K. Sato, S. Fujita, K. Suzuki, T. Mori, High performance of Ni-substituted calcium aluminosilicate for partial oxidation of methane into syngas, Catalysis Communications, 8 (2007) 1735-1738.

[86] G.P. Berrocal, A.L.M.D. Silva, J.M. Assaf, A. Albornoz, M.d.C. Rangel, Novel supports for nickel-based catalysts for the partial oxidation of methane, Catalysis Today, 149 (2010) 240-247.

[87] B.S. Liu, C.T. Au, Carbon deposition and catalyst stability over La_2NiO_4/γ-Al_2O_3 during CO_2 reforming of methane to syngas, Applied Catalysis A: General, 244 (2003) 181-195.

[88] C. Alvarez-Galvan, M. Melian, L. Ruiz-Matas, J.L. Eslava, R.M. Navarro, M. Ahmadi, B. Roldan Cuenya, J.L.G. Fierro, Partial Oxidation of Methane to Syngas Over Nickel-Based Catalysts: Influence of Support Type, Addition of Rhodium, and Preparation Method, Frontiers in Chemistry, 7 (2019).

[89] S. Tang, J. Lin, K.L. Tan, Partial oxidation of methane to syngas over Ni/MgO, Ni/CaO and Ni/CeO_2, Catalysis Letters, 51 (1998) 169-175.

[90] G. Pantaleo, V.L. Parola, F. Deganello, R.K. Singha, R. Bal, A.M. Venezia, Ni/CeO_2 catalysts for methane partial oxidation: Synthesis driven structural and catalytic effects, Applied Catalysis B: Environmental, 189 (2016) 233-241.

[91] R.K. Singha, A. Shukla, A. Yadav, L.N. Sivakumar Konathala, R. Bal, Effect of metal-support interaction on activity and stability of Ni-CeO_2 catalyst for partial oxidation of methane, Applied Catalysis B: Environmental, 202 (2017) 473-488.

[92] M. Peymani, S.M. Alavi, M. Rezaei, Preparation of highly active and stable nanostructured Ni/CeO_2 catalysts for syngas production by partial oxidation of methane, International Journal of Hydrogen Energy, 41 (2016) 6316-6325.

[93] J. Hu, C. Yu, Y. Bi, L. Wei, J. Chen, X. Chen, Preparation and characterization of Ni/CeO_2-SiO_2 catalysts and their performance in catalytic partial oxidation of methane to syngas, Chinese Journal of Catalysis, 35 (2014) 8-20.

[94] L. Cao, Y. Chen, W. Li, Effect of La2O3 added to NiO/Al_2O_3 catalyst on partial oxidation of methane to syngas, in: M. de Pontes, R.L. Espinoza, C.P. Nicolaides, J.H. Scholtz, M.S. Scurrell (Eds.) Studies in Surface Science and Catalysis, Elsevier1997, pp. 467-471.

[95] M.G. González, N.N. Nichio, B. Moraweck, G. Martin, Role of chromium in the stability of Ni/Al_2O_3 catalysts for natural gas reforming, Materials Letters, 45 (2000) 15-18.

[96] H.-t. Wang, Z.-h. Li, S.-x. Tian, Effect of promoters on the catalytic performance of Ni/Al_2O_3 catalyst for partial oxidation of methane to syngas, Reaction Kinetics and Catalysis Letters, 83 (2004) 245-252.

[97] A.C. Ferreira, A.M. Ferraria, A.M.B. do Rego, A.P. Gonçalves, M.R. Correia, T.A. Gasche, J.B. Branco, Partial oxidation of methane over bimetallic nickel–lanthanide oxides, Journal of Alloys and Compounds, 489 (2010) 316-323.

[98] W. Cho, H. Yu, W.-S. Ahn, S.-S. Kim, Synthesis gas production process for natural gas conversion over Ni–La_2O_3 catalyst, Journal of Industrial and Engineering Chemistry, 28 (2015) 229-235.

[99] D. Kaddeche, A. Djaidja, A. Barama, Partial oxidation of methane on co-precipitated Ni–Mg/Al catalysts modified with copper or iron, International Journal of Hydrogen Energy, 42 (2017) 15002-15009.

[100] C. Cheephat, P. Daorattanachai, S. Devahastin, N. Laosiripojana, Partial oxidation of methane over monometallic and bimetallic Ni-, Rh-, Re-based catalysts: Effects of Re addition, co-fed reactants and catalyst support, Applied Catalysis A: General, 563 (2018) 1-8.

[101] K.O. Christensen, D. Chen, R. Lødeng, A. Holmen, Effect of supports and Ni crystal size on carbon formation and sintering during steam methane reforming, Applied Catalysis A: General, 314 (2006) 9-22.

[102] H.S. Bengaard, J.K. Nørskov, J. Sehested, B.S. Clausen, L.P. Nielsen, A.M. Molenbroek, J.R. Rostrup-Nielsen, Steam Reforming and Graphite Formation on Ni Catalysts, Journal of Catalysis, 209 (2002) 365-384.

[103] A.R.K. Gollakota, V. Volli, C.M. Shu, Progressive utilisation prospects of coal fly ash: A review, Sci Total Environ, 672 (2019) 951-989.

[104] S.R. Wang, F. Zhang, Q.J. Cai, X.B. Li, L.J. Zhu, Q. Wang, Z.Y. Luo, Catalytic steam reforming of bio-oil model compounds for hydrogen production over coal ash supported Ni catalyst, International Journal of Hydrogen Energy, 39 (2014) 2018-2025.

[105] M. Shahbaz, S. Yusup, A. Inayat, D.O. Patrick, A. Pratama, M. Ammar, Optimization of hydrogen and syngas production from PKS gasification by using coal bottom ash, Bioresour Technol, 241 (2017) 284-295.

[106] A.S. Al-Rahbi, P.T. Williams, Waste ashes as catalysts for the pyrolysis–catalytic steam reforming of biomass for hydrogen-rich gas production, Journal of Material Cycles and Waste Management, 21 (2019) 1224-1231.

Chapter 3

Experimental Work

3.1 Material and Method

3.1.1 Preparation of BFA

The sample preparation for BFA is presented in Figure 3-1(a). Initially, the dried sample is grinded in Hard Grove Grindability Index Tester (USA, ASTM D 409–08). The material was then sieved in a WS Tyler RX-29–10 (USA) sieving machine to obtain the fine powder. To eliminate the contaminants, the samples were cleaned with ethanol and deionized (DI) water. After washing, the material was dried, grinded then calcined for 4 hours at 850 degrees Celsius to increase purity and crystallinity.

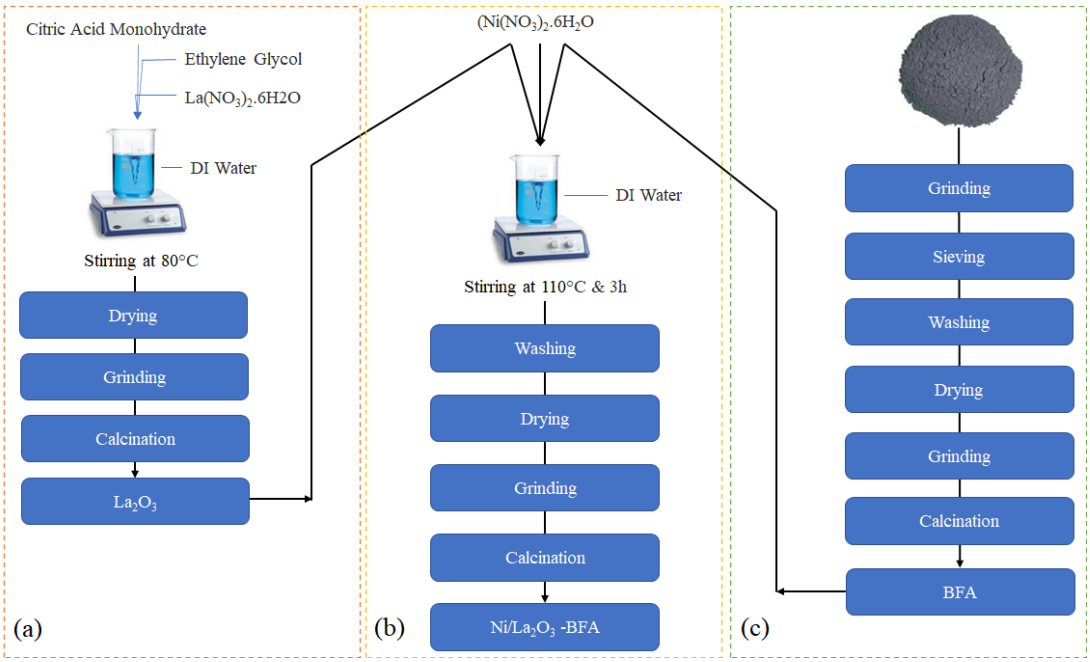

Figure 3-1 Schematic of material synthesis

3.1.1 Preparation of La_2O_3

La_2O_3 was prepared by the sol-gel method [1] as presented in Figure 3-1(c). In deionized water, $La(NO_3)_2.6H_2O$, citric acid monohydrate, and ethylene glycol were dissolved with a 1:2:2 stoichiometric molar ratio. The solution was continually stirred at 80°C to generate a thick gel. The gel was then dried at 110 °C, grinded and then calcined at 850 °C for 4 h.

3.1.1 Preparation of Ni/ La_2O_3-BFA

Ni/La_2O_3-BFA was synthesized by incipient wet impregnation method [2] as shown in Figure 3-1(b). Nickel (II) nitrate hexahydrate ($Ni(NO_3)_2.6H_2O$) Sigma Aldrich) solution (0.1 M) was made using DI water at 60°C for 10 minutes while stirring constantly. Then BFA and La_2O_3 promoter were added with the ratio of 9:1 by (%) at 110 ℃ to precursor and then stirred continuously for 3 hours. The sample was rinsed with DI water after stirring and dried in the oven overnight at 110 °C. The catalyst was then calcined for 4 hours at 850°C.

3.2 Catalyst Characterisation

3.2.1 X-Ray Diffraction

The catalysts (XRD) patterns were acquired by D8 Advance (Bruker Advanced, Germany) equipped with a Bragg-Brentano configuration and scintillation detector with a radiation wavelength of 1.5418 Å. Based on diffraction patterns different compounds were characterized in this technique. With a step size of.05°/5s, different samples were scanned ranging from 2θ= 10° to 80°. DIFFRAC Plus EVA Version 5.0 was utilized to examine the XRD analysis.

Figure 3-2 X-Ray Diffraction

3.2.3 Scanning Electron Microscopy

SEM was used to investigate the morphological parameters of the fresh and spent catalysts using a JEOL JSM-6490A. (Japan). The elemental composition of the fresh and spent catalysts was determined using an EDX detector (Oxford Instruments, model 52-AD0007).

Figure 3-3 Scanning Electron Microscopy

3.2.4 Thermogravimetric analysis

Thermal stability was determined by TGA 500 (TA Instruments, USA). The sample was purged by the N_2 flow rate of 35 mL min^{-1} for 30 min. The sample was heated up to 900 ℃ with a heating rate of 10 ℃/min under O_2.

Figure 3-4 Thermogravimetric Analyzer

3.2.5 Fourier Transform Infrared Spectroscopy

The infrared spectra absorption ranges between 4000 to 650 cm^{-1} having a resolution of 2 cm^{-1} were scanned utilizing Cary 630 (Agilent Technologies, USA) to investigate the functional groups.

Figure 3-5 Fourier Transform Infrared Spectroscopy.

3.3 Partial Oxidation of Methane Experimental Setup

The synthesized catalysts' catalytic performance was tested in a fixed bed reactor (Parr Instrument, 5401, USA) presented in Figure 3-6. The fixed-bed reactor with a single zone heating furnace made of stainless steel (SS-316) tube having the dimension of 300 mm in length with inner and outer diameter of 12 mm and 14 mm, respectively. The prepared catalyst 0.3 gram was sandwiched in quartz wool and placed in the heating zone of the reactor. The reactor temperature was set at 850 ℃ through a process controller (4871, Parr Instrument) [3]. Mass flow controller (Brooke instruments, USA) was used to regulate the flow rate of CH_4 (99.99%) and O_2 (99.99%) with a ratio of 2:1. An online SCADA system was employed to keep track of the temperature and flow rate of the reactor. Before starting the reaction, the catalysts were reduced with H_2 at a flow rate of 30mL/min for 1 hour at 750 ℃. A condenser was utilized at the reactor's output to remove moisture and provide dry product gases for examination in gas chromatograph (GC-TCD) (GC-2010 Pro, Shimadzu Japan) having a thermal conductivity detector (TCD) and capillary column (RT-MS5A, 30 m×0.3 mm ID, 30 µm) [4] to detect CH_4, CO, H_2 and CO_2.

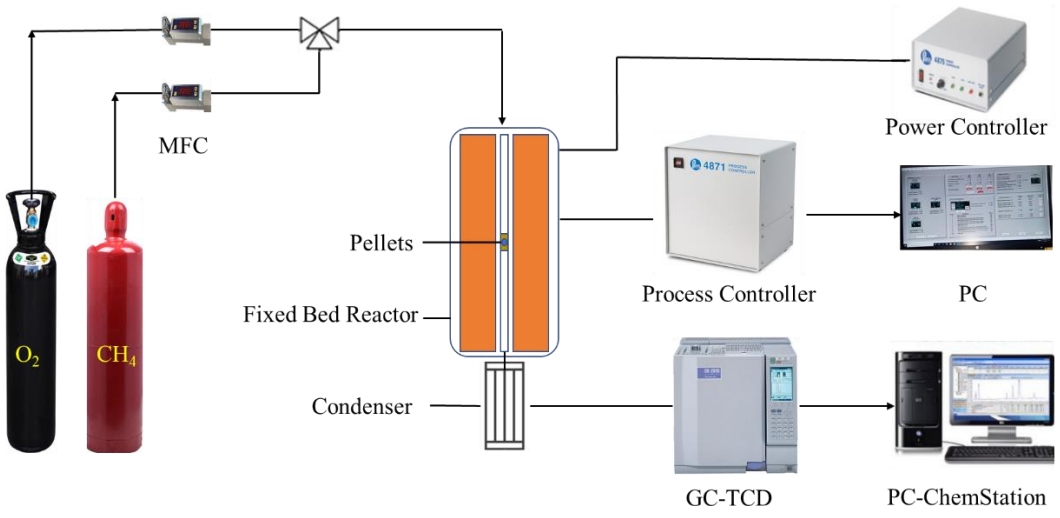

Figure 3-6 Schematic of the experimental setup for POM.

3.4 Partial Oxidation of Methane Catalytic Activity Calculations

The catalytic activity of the catalyst for POM was analyzed based on CH_4 conversion (Eq. 3), H_2 selectivity (Eq. 4) and CO selectivity (Eq. 5) and H_2/CO ratio (Eq. 6).

$$CH_4 \text{conversion}\left(X_{CH_4}\right)\% = \left[\frac{(n\ CH_4)_{converted}}{(n\ CH_4\ )_{feed}} \times 100\right] \quad \text{Eq 3}$$

$$H_2\ \text{selectivity}\left(S_{H_2}\right)\% = \left[\frac{(nH_2)_{produced}}{(2 \times nCH_4)_{converted}} \times 100\right] \quad \text{Eq 1}$$

$$\text{CO selectivity}\left(S_{CO}\right)\% = \left[\frac{(nCO)_{produced}}{(nCH_4)_{converted}} \times 100\right] \quad \text{Eq 2}$$

$$H_2/\text{CO ratio} = \left[\frac{\text{selectivity}(S_{H_2})}{\text{selectivity}(S_{CO})}\right] \quad \text{Eq 3}$$

References

[1] L. Liu, Z. Zhang, S. Das, S. Xi, S. Kawi, $LaNiO_3$ as a precursor of Ni/La_2O_3 for reverse water-gas shift in DBD plasma: Effect of calcination temperature, Energy Conversion and Management, 206 (2020) 112475.

[2] A.H. Khoja, M. Tahir, N.A.S. Amin, Cold plasma dielectric barrier discharge reactor for dry reforming of methane over Ni/γ-Al_2O_3-MgO nanocomposite, Fuel Processing Technology, 178 (2018) 166-179.

[3] A. Zaffar, B.A. Khan, A.H. Khoja, U.M. Khan, Q. Sarmad, M.T. Mehran, S.R. Naqvi, M. Ali, Synthesis of Ash Derived Co/Zeolite Catalyst for Hydrogen Rich Syngas Production via Partial Oxidation of Methane, 2021, (2021).

[4] J. Raza, A.H. Khoja, S.R. Naqvi, M.T. Mehran, S. Shakir, R. Liaquat, M. Tahir, G. Ali, Methane decomposition for hydrogen production over biomass fly ash-based CeO_2 nanowires promoted cobalt catalyst, Journal of Environmental Chemical Engineering, (2021) 105816.

Chapter 4

Results and Discussion

4.1 Materials Characterization

4.1.1 XRD Analysis

X-ray diffraction (XRD) experiments were made to analyze the structure of the prepared catalyst as shown in Figure 4-1. BFA's XRD exhibits a variety of peaks for various metals oxides such as $CaCO_3$ (JCPDF#47-1743) at 2θ=29.4° with rhombohedral phase (hkl;104) [1]. SiO_2 (JCPDF#46-1045) at 26.5° with (hkl;101) [2]. Al_2O_3 (JCPDF#46-1131) is identified at 2θ=30.3° with (hkl; 020) [3]. Fe_2O_3 (JCPDF#16-0653) is scanned at 2θ=33° with cubic phase (hkl; 220) [4]. MgO (JCPDF#45-0946) is found at 2θ=44° with cubic phase (hkl;211) [5]. The XRD of La_2O_3 has a major peak matched at 2θ=27.24° with (space group Ia3, JCPDF#22-0369) cubic phase (hkl;222) and is well-supported by the literature[6]. The XRD of Ni/La_2O_3-BFA catalyst shows peaks for $LaNiO_3$ (JCPDF#33-0710) at 2θ=23° with a cubic phase (hkl;100) [7]. The La_2NiO_4(JCPDF#11-0557) is found at 2θ=31° with a tetragonal phase (hkl;103)[8]. $NiAl_2O_4$(JCPDF#71-0963) is also formed and scanned at 2θ=49° with spinel phase (hkl;311) [9]. while NiO (JCPDF#44-1159) is presented at 2θ=43.2° with hexagonal phase (hkl;101) [10] and La_2O_3 (space group Ia3, JCPDF#22-0369) peak at 27.24° with cubic phase (hkl;222) [6].

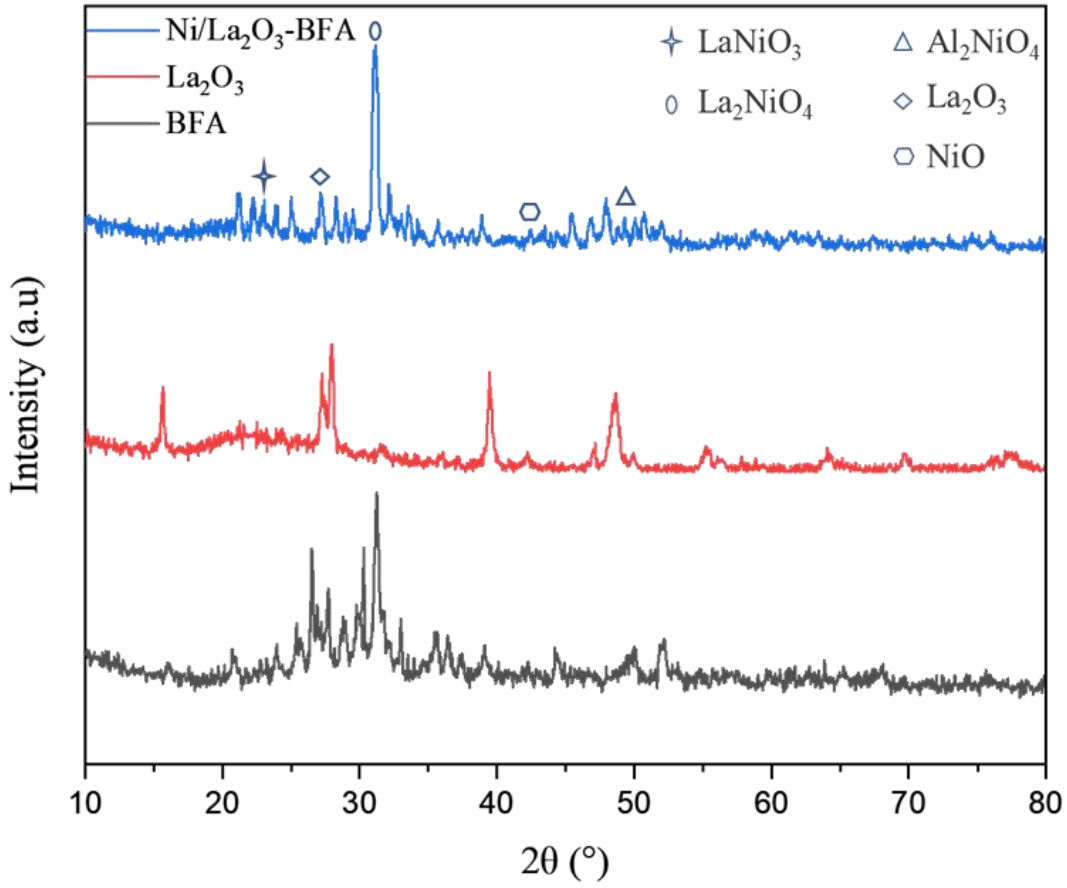

Figure 4-1 XRD of synthesized catalysts

4.1.2 SEM Analysis

SEM was used to examine the morphology of BFA, La_2O_3, and Ni/La_2O_3-BFA, as shown in Figure 4-2. For all samples, the field magnification is set at 5.0 µm and 1.0 µm. The BFA SEM micrograph shows agglomerated irregular shape particles with amorphous structure as demonstrated in Figure 4-2(a-b) [11]. La_2O_3 micrograph with different field magnification is depicted in Figure 4-2(c-d). It shows the platelet like structure of different sized agglomerated particles[12] [13]. The final composite 5%Ni/La_2O_3-BFA micrograph Figure 4-2(e-f) shows a compact aggregation of La_2O_3 particles over BFA support [14].

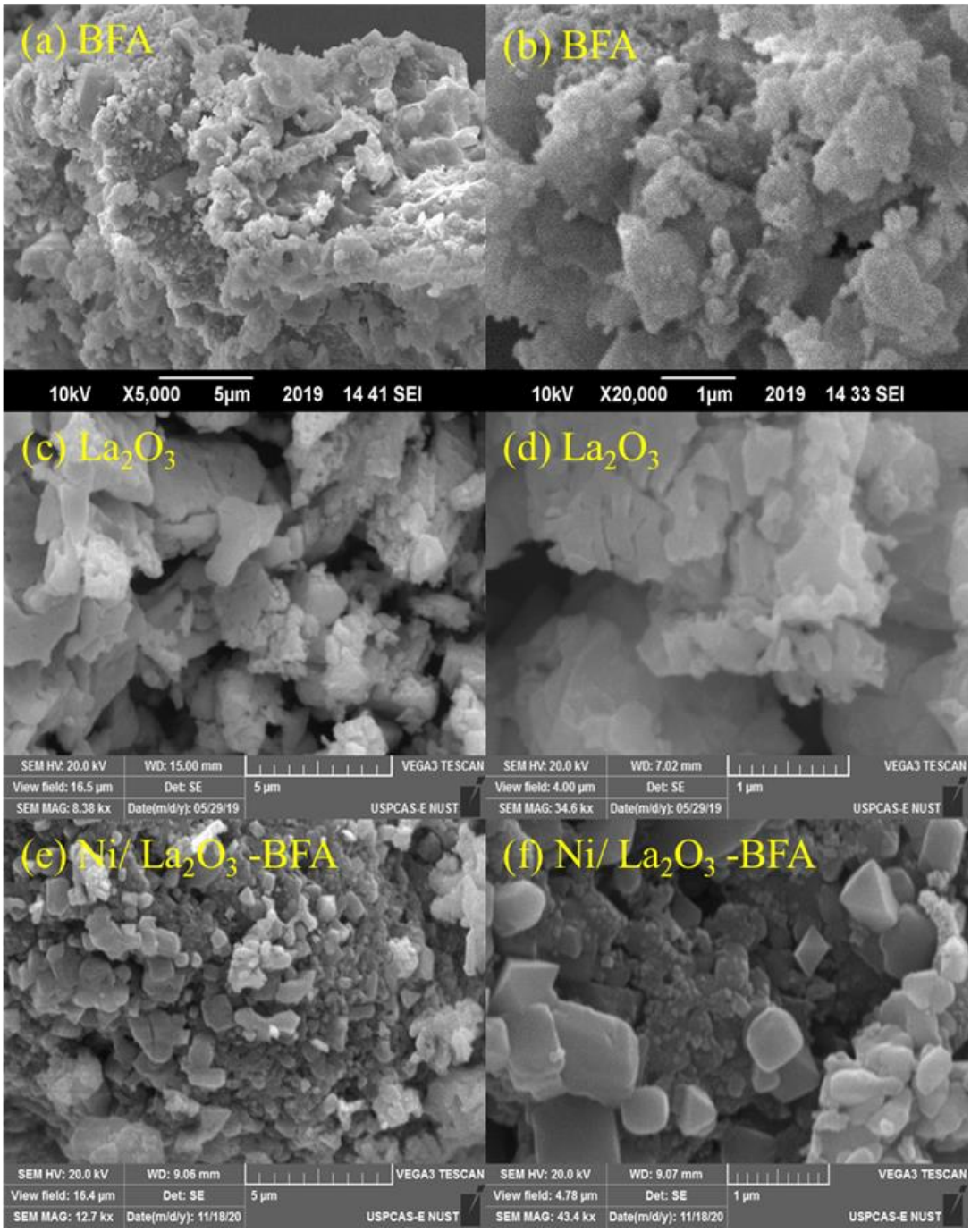

Figure 4-2 SEM micrographs of synthesized catalyst with 5.0 μm and 1.0 μm (a-b) BFA (c-d) La_2O_3 (e-f) Ni/ La_2O_3-BFA

4.1.3 EDX Analysis

The elemental analysis of 5%Ni/La_2O_3-BFA was performed using the EDX technique as shown in Figure 4-3. La and Ni are better dispersed over BFA due to their porous nature and multiple oxides. In the EDX spectrum, there are distinct Ni and La peaks. Peaks for Ca, Si, Fe, and Al can also be seen in the EDX spectrum, indicating that these minerals are present in BFA, as confirmed by the XRD.

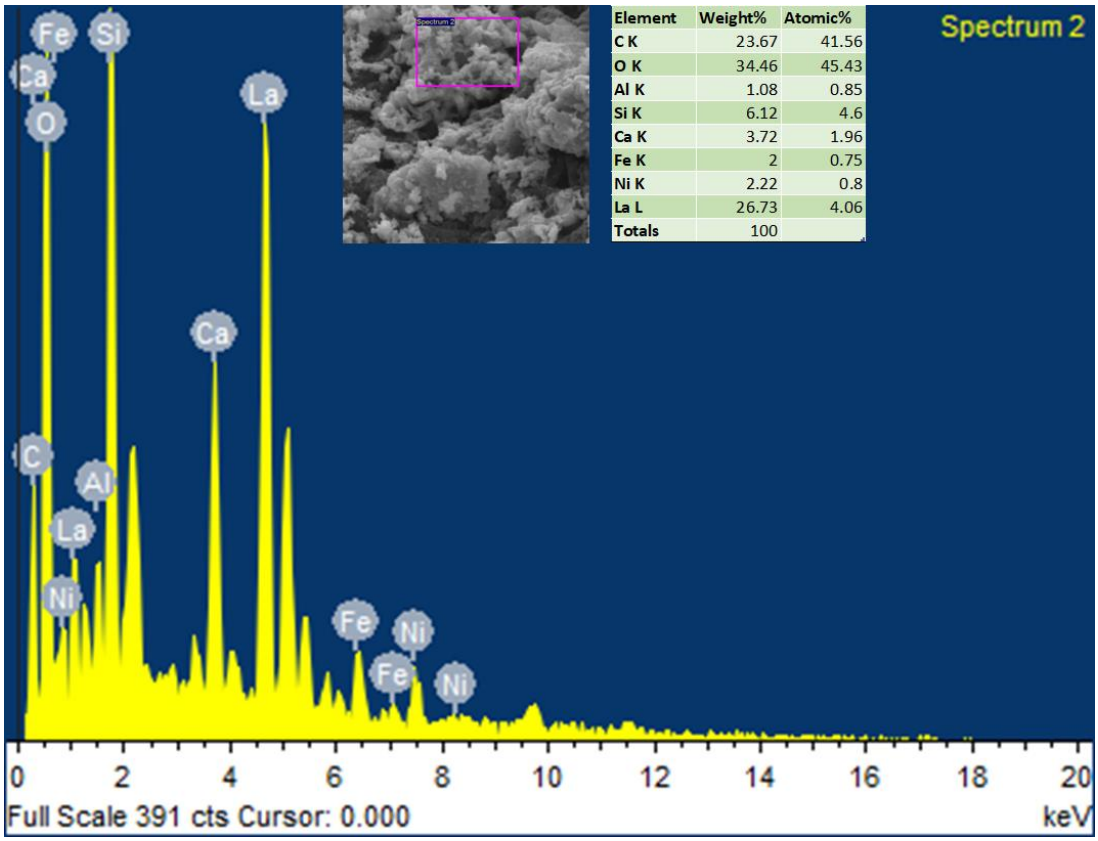

Figure 4-3 EDX analysis of fresh Ni/La_2O_3-BFA

4.1.4 TGA Analysis

The thermal stability of BFA, La_2O_3-BFA, and 5%Ni/La_2O_3-BFA is illustrated in Figure 4-4. The thermal stability of BFA is shown in Figure 4-4(a) which depicts a minute weight loss below 200 °C due to evaporation of moisture content. The weight loss between 200 and 600 degrees relates to the evaporation of other volatile substances. From 600 °C to 900 °C major weight loss is because of phase transfer and oxidation of organic material [11]. The total weight loss recorded in this sample is about 15%.

Figure 4-4(b) Shows thermal stability of La_2O_3. The elimination of carbonaceous molecules causes the first weight loss between 150 and 350 °C while the remaining weight loss after 350 °C is due to the decomposition of an organic material having covalent bonds. The total weight loss recorded in this sample is about 4%. In the case of 5%Ni/La_2O_3-BFA, as depicted in Figure 4-4(c), there is a slight weight loss of 0.08% before 200 °C due to the desorption of water. The 0.7% weight loss between 200°C to 900°C can be ascribed to Ni reduction [15]. In the synthesized sample there is little weight loss because the Ni impregnation over La_2O_3 promoted BFA support changed the morphology and strengthen the stability of the synthesized sample [16, 17].

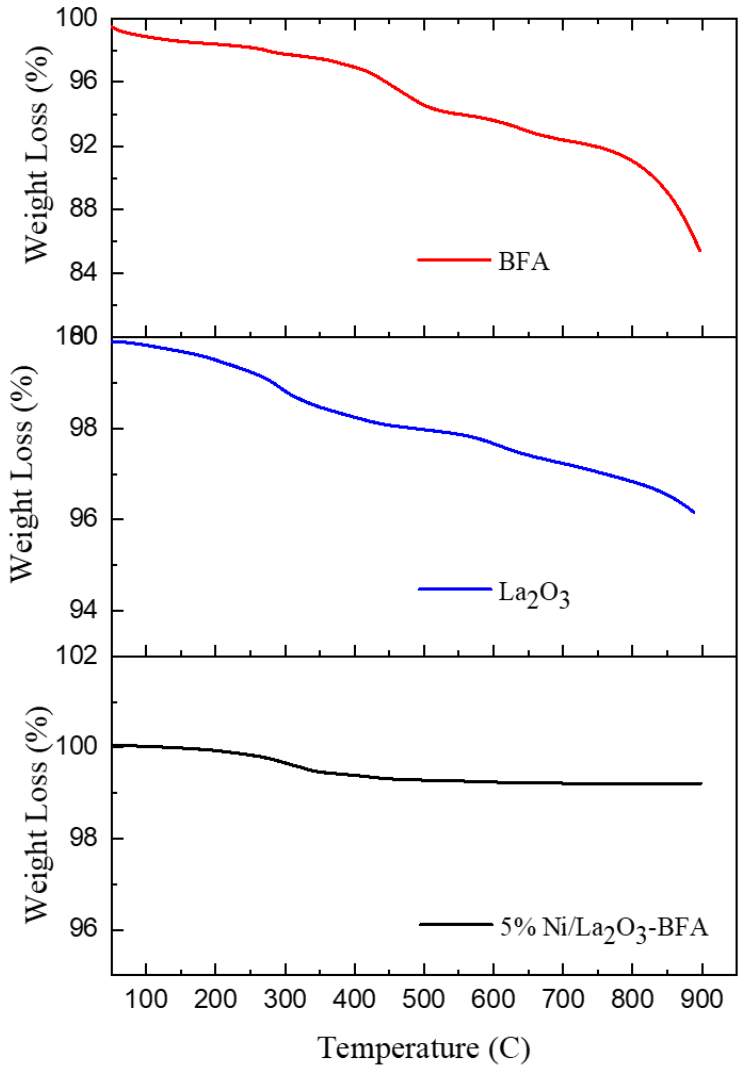

Figure 4-4 TGA profile of fresh (a) BFA (b) La_2O_3 (c) Ni/La_2O_3-BFA

4.1.5 FTIR Analysis

The FTIR spectrum of the prepared catalyst between 4500-500 cm $^{-1}$ wavenumber is presented in Figure 4-5. FTIR spectrum of BFA shows a band at 1110 cm $^{-1}$ corresponds to Si-O stretching vibration [11, 18]. La_2O_3 shows bands between 1350-1500 cm $^{-1}$ due to ions vibrations and frequencies between 1000-600 cm $^{-1}$ confirm La_2O_3 presence [19]. In 5%Ni/La_2O_3-BFA spectrum absorption peak at around 1000 cm $^{-1}$ was observed for asymmetric vibration of Si-O-Al. Another band at a relatively smaller neck between 700-600 cm $^{-1}$ is ascribed to stretching vibration of Ni-O [20].

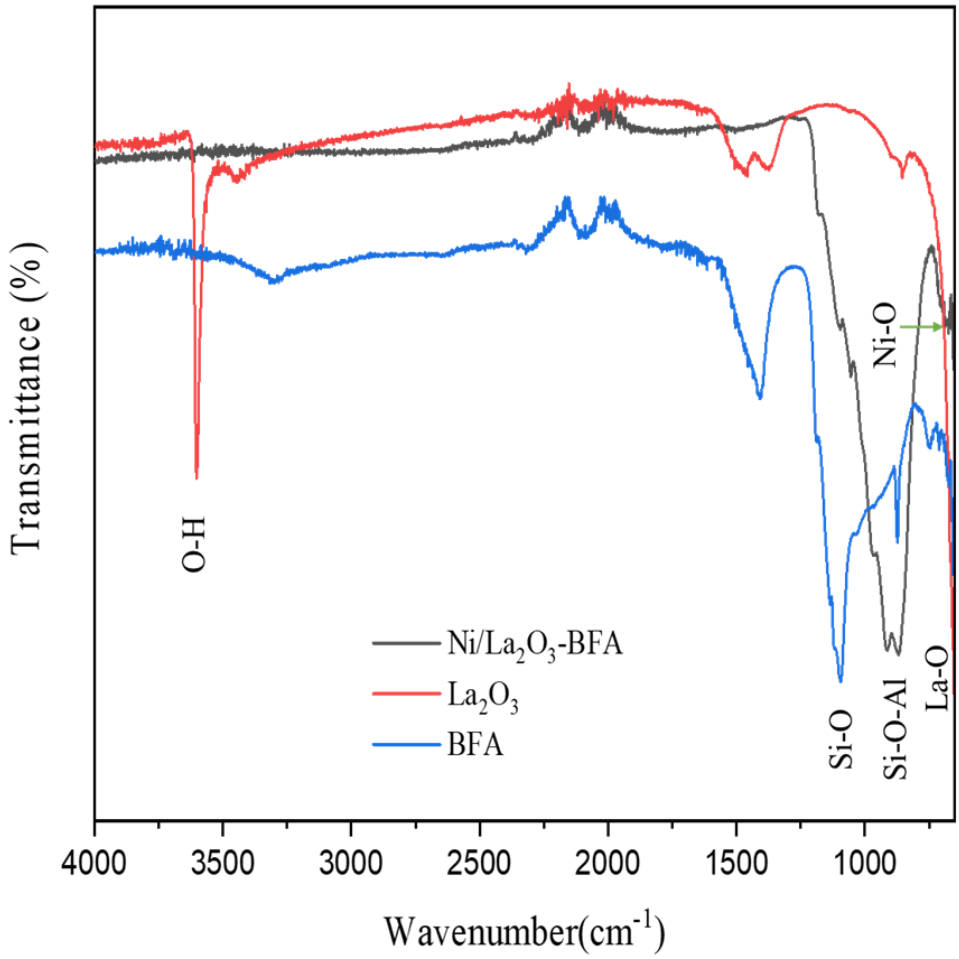

Figure 4-5 FTIR spectrum of the synthesized catalyst

4.2 POM Catalytic Activity Analysis

4.2.1 Catalyst Screening Test

All the prepared catalysts i.e., BFA, La_2O_3-BFA, 5%Ni/La_2O_3-BFA and 10%Ni/La_2O_3-BFA were assessed in a FBR for POM to investigate the catalytic activity in terms of CH_4 conversion and H_2/CO ratio. The experimental conditions such as temperature= 850 ℃, CH_4 flowrate=20 ml min^{-1}, O_2 flowrate=10 ml min^{-1} keeping the ratio 2:1, and catalyst loading of 0.3gm was kept constant during a screening test.

All the reported values in Figure 4-6 are the average values taken after catalyst activity become stable. From Figure 4-6(a) CH_4 conversion value for BFA catalyst is (55%) but the addition of La_2O_3 promotor to BFA support increased the CH_4 conversion to 65% since La_2O_3 facilitate carbon gasification [15], give strong basic nature [21] and La_2O_3 react with CO_2 to produce $La_2O_2CO_3$ confirmed by XRD [22]. The addition of 5% Ni as an active metal to the final catalyst increased the CH_4 conversion values from (65%) to (85%) this is because Ni stimulates methane decomposition and increases active sites. Further addition of 5%Ni to 5%Ni/La_2O_3-BFA increased CH_4 conversion from 85% to 87 % that is not significant because the catalytic properties are not proportional to Ni loading as reported [23]. The trend observed for CH_4 conversion in Figure 4-6(a) is also depicted in H_2 and CO selectivity. H_2 selectivity values for BFA, La_2O_3-BFA, 5% Ni/La_2O_3-BFA and 10% Ni/La_2O_3-BFA are 35%, 37%, 41% and 43% respectively as presented in Figure 4-6(b). In Figure 4-6(c) CO selectivity values for BFA, La_2O_3-BFA, 5% Ni/La_2O_3-BFA and 10% Ni/La_2O_3-BFA are 21%, 20%, 20% and 32% respectively. Figure 4-6(d) shows H_2/CO ratio for BFA, La_2O_3-BFA, 5% Ni/La_2O_3-BFA and 10% Ni/La_2O_3-BFA which are 1.6, 1.8, 2 and 1.4, respectively.

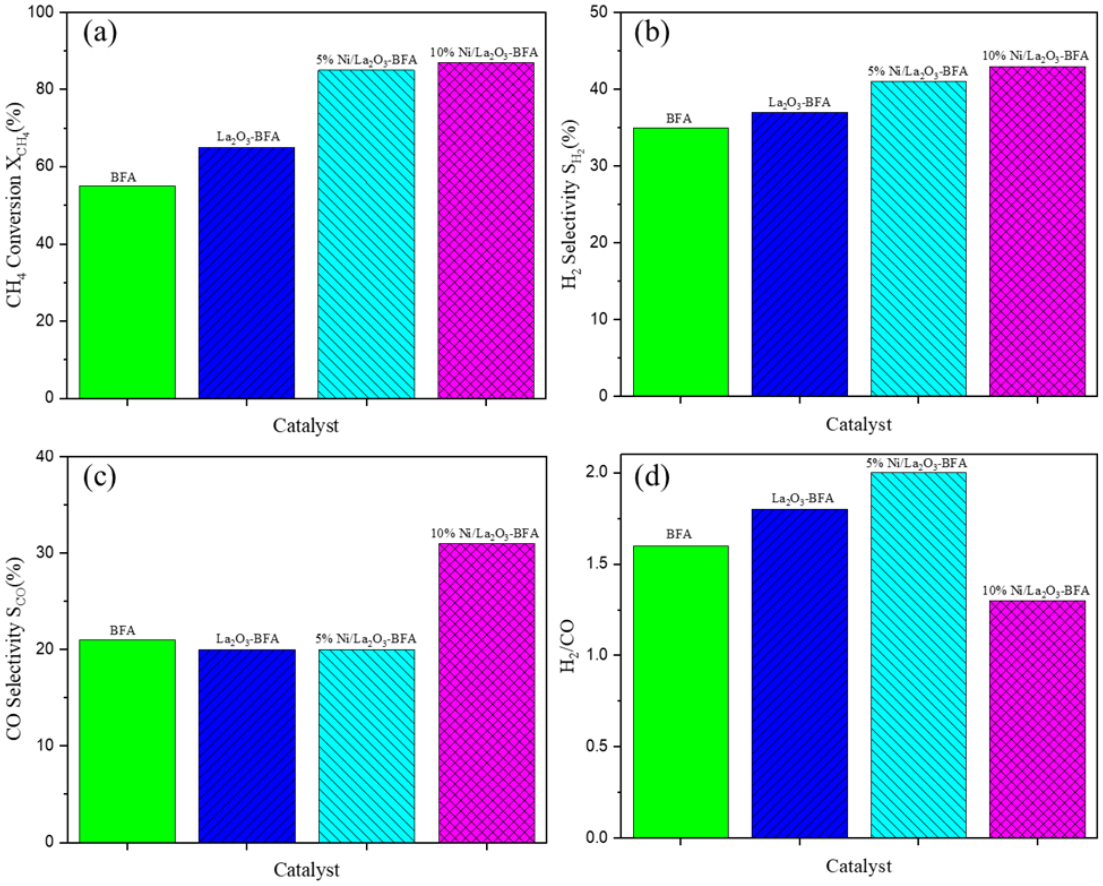

Figure 4-6 Catalyst Screening (a) CH_4 Conversion (b) H_2 Selectivity (c) CO Selectivity (d) H_2/CO ratio: catalyst loading=0.3g, reaction temperature 850°C, feed flow rate of CH_4/O_2=20/10 mL min^{-1}

The prepared catalyst screening was performed on POM for 8.5 hours (TOS) as shown in Figure 4-7 as mentioned earlier the maximum increase in CH_4 conversion Figure 4-7(a) was reported for 5% Ni/La_2O_3-BFA which is 85%. 10% Ni/La_2O_3-BFA gives a higher value for CH_4 conversion Figure 4-7(a) but the increase in values is not significant as it is in 5% Ni/La_2O_3-BFA because increasing Ni loading may result in Ni particle agglomeration[24] due to which results may not increase in proportion to Ni loading [23]. In Figure 4-7(b) H_2/CO are shown in which 5% Ni/La_2O_3-BFA has a ratio of 2 while 10% Ni/La_2O_3-BFA has the lowest ratio of 1.4. The decrease in the ratio may be due to $La_2O_2CO_3$ at the interface between Ni and La_2O_3. $La_2O_2CO_3$ attacks the carbon species deposited over increased Ni sites closer to La_2O_3 or LaO_x species that result in higher production of CO [25] thus reduces H_2/CO ratio. The presence of basic oxides such as SiO_2, Al_2O_3, Fe_2O_3, MgO in BFA provides the benefits of multi metallic supports however the visible phase formed due to metallic

oxide in BFA is $NiAl_2O_4$ spinel phase confirmed by XRD. That is formed by the reaction of Al_2O_3 with Ni. $NiAl_2O_4$ suppress carbon deposition [26], resist catalyst sintering and aggregation [27]. The La_2NiO_4 and $LaNiO_3$ phase confirmed by XRD decompose into Ni particles and La_2O_3 providing Ni actives site that resists sintering [27]. The $NiAl_2O_4$, La_2NiO_4 and $LaNiO_3$ phases detected by XRD depicts good interaction between the Ni active metal, BFA support and La_2O_3 promoter. The overall catalytic results for 5% Ni/La_2O_3-BFA are good thus paving the way for further stability analysis of 5% Ni/La_2O_3-BFA.

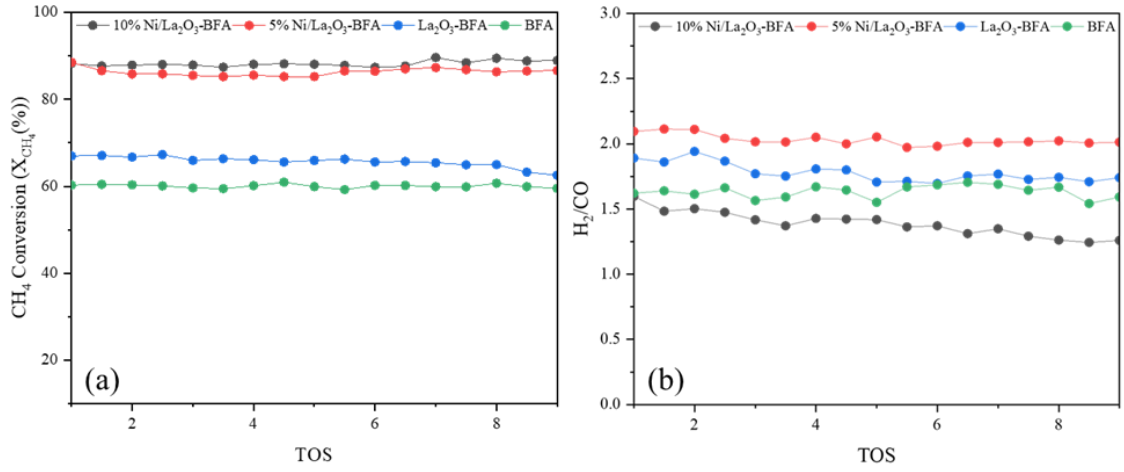

Figure 4-7 Effect of time on stream (TOS) on a) CH_4 Conversion (b) H_2/CO: catalyst loading=0.3g, reaction temperature 850 °C, feed flow rate of CH_4/O_2=20/10 mL min^{-1}

4.2.4 Stability Analysis of 5% Ni/La_2O_3-BFA

The stability analysis that was completed for 5% Ni/La_2O_3-BFA is shown in Figure 4-8. 5% Ni/La_2O_3-BFA catalyst was put on test for 30h time on stream (TOS) while the test parameters were kept constant. The CH_4 conversion and H_2/CO ratio are shown in Figure 4-8. Catalytic activity increased several hours due to the induction period that can be attributed to solid-state reactions in the catalysts. [28, 29] or Ni particle activation [30]. After few hours the catalytic activity becomes stable on stream with CH_4 conversion of 85% and H_2/CO ratio of about 2 which is optimal for FT process [31]. It could be observed that excellent stability was exhibited by the 5% Ni/La_2O_3-BFA in the reported TOS of 30h without deactivation which is encouraging for the final catalyst. The stability of 5% Ni/La_2O_3-BFA is due to the availability of a spinal structure of $NiAl_2O_4$ phase that prevents aggregation of Ni particles [27] while

La_2O_3 addition enhanced metal support interaction confirmed by the presence of $NiAl_2O_4$ and La_2NiO_4 phases and CO_2 adsorption on La_2O_3 or LaO_x species in form of $La_2O_2CO_3$ that decorates Ni sites. Carbon species deposited over Ni sites are removed by oxygen from $La_2O_2CO_3$ thus ensuring stable and active performance[32]. The prevalence of several metal oxides in BFA, as well as their interactions with Ni and La_2O_3 can be confirmed by the presence of $NiAl_2O_4$, La_2NiO_4 and $LaNiO_3$ phases in XRD which contribute to the structural stability, reduces to Ni that is resistant to sintering and La_2O_3 that impart basic nature. The irregular structure of BFA support confirmed by SEM respectively increase the dispersion, stabilize and enhance active sites through the metal exsolution process which increase the catalytic activity.

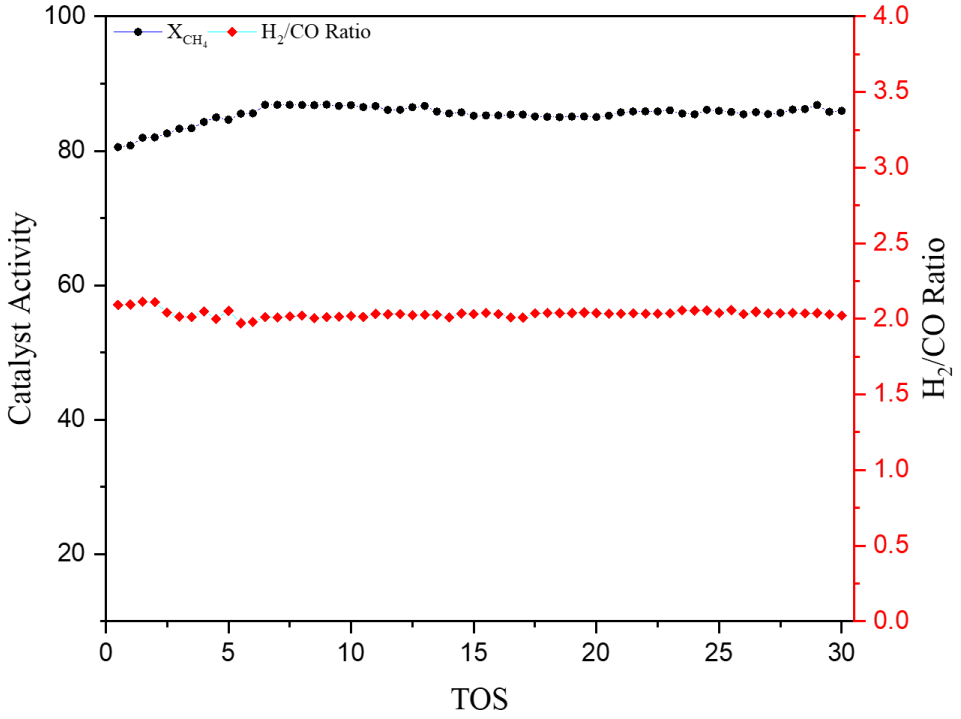

Figure 4-8 Effect of 5% Ni/La_2O_3 time on stream (TOS) CH_4 conversion and H_2/CO ratio: catalyst loading=0.3g, reaction temperature 850°C, feed flow rate of CH_4/O_2=20/10 $mLmin^{-1}$

The presence of different oxides in the BFA support confirmed by XRD [11] such as SiO_2, Fe_2O_3, Al_2O_3 and MgO enhanced catalytic performance by enhancing catalyst stability as represented by the CH_4 conversion and H_2/CO ratio thus making BFA a good alternative to other commercially available supports whose cost and complex synthesis is a major issue. Due to the existence of several metal oxides in

BFA, it is difficult to correlate the impact of specific metals on the catalytic performance of the catalyst.

A comparison of the previously studied catalyst for POM with the present study is presented in Table 4.1. The comparison of the newly reported waste-derived catalyst with a previously reported catalyst in the literature makes the competitiveness of the waste-derived catalyst apparent. The point-to-point comparison is not possible due to the different experimental and reactor configurations.

Table 4.1 Literature comparison for POM reactions to the present study

Catalyst	**XCH_4 (%)**	**H_2/CO ratio**	**Reaction Condition**	**Ref**
5% Ni/La_2O_3-BFA	85	2.0	T = 850 °C Catalyst loading = 0.3 g	Present work
Pt (2 wt%)/Al_2O_3	78	-	T = 800 °C Catalyst loading = 40 mg	[33]
Al_2NiO_4 (Ni/Al = 0.25)	81	2.3	T = 700 °C, Catalyst loading = 0.125 g	[34]
5% Co/Al_2O_3-ZrO_2	84	2.2–2.3	T = 800 °C, Catalyst loading = 0.15 g	[35]
12La30Ni	88.6	1.9	T = 800 °C, Catalyst loading = 180 mg	[36]
Ni/Al_2O_3+Mg	92	-	T = 650 °C Catalyst loading = 100 mg	[37]

4.2.5 Reaction Mechanism

The possible main reaction routes to products and catalyst generation being presented in a series of reactions below. In the initial stage, Ni is oxidized to NiO (R14). After Ni oxidation, the complete oxidation of CH_4 to a certain extinct take place over NiO along with reduction of NiO to Ni by CH_4 that lead to the formation of H_2O and CO_2 (R15 – R16). The reduced Ni further react with CH_4 forming Ni-C surface species and H_2 (R17). The CO_2 produced during complete oxidation is adsorbed by La_2O_3 forming $La_2O_2CO_3$ (R18). The formed Ni-C species may further react with $La_2O_2CO_3$ to produce CO along with the regeneration of La_2O_3 and Ni (R19). The

reaction is only proposed for Ni-La interactions however, the multiple oxides will assist the adsorption of reactant gases.

$$Ni^0 + O_2 \rightarrow NiO \quad \text{(R 14)}$$

$$CH_4 + O_2 \rightarrow CO_2 + H_2O \quad \text{(R 15)}$$

$$CH_4 + NiO \rightarrow CO_2 + H_2O + Ni^0 \quad \text{(R 16)}$$

$$CH_4 + Ni^0 \rightarrow Ni - C + 2H_2 \quad \text{(R 17)}$$

$$CO_2 + La_2O_3 \rightarrow La_2O_2CO_3 \quad \text{(R 18)}$$

$$La_2O_2CO_3 + Ni - C \rightarrow Ni + La_2O_3 + CO \quad \text{(R 19)}$$

4.3 Characterization of Spent Catalyst

4.3.1 XRD Analysis

The spent catalyst's XRD is illustrated in Figure 4-9(a). XRD confirmed the presence of graphite carbon (COD No. 96-901-2236) at 30.3°, 31.63°,33.8°,37.39° and 42° with phase (hkl; 002), (hkl; 020), (hkl; 021) [38]respectively. NiO (card No. 96-101-0094) at 43.42 with phase (hkl;200)[39]. $La_2O_2CO_3$ at 30.3° with hexagonal phase (hkl;103) [40]. La_2O_3 (JCPDF#22-0369) cubic structure (hkl; 222) was detected at 27.15° (hkl; 222) [6]. The presence of La_2O_3 in its pure form represents its thermal stability even though the catalyst was heated at 850℃ for 30h in the reactor.

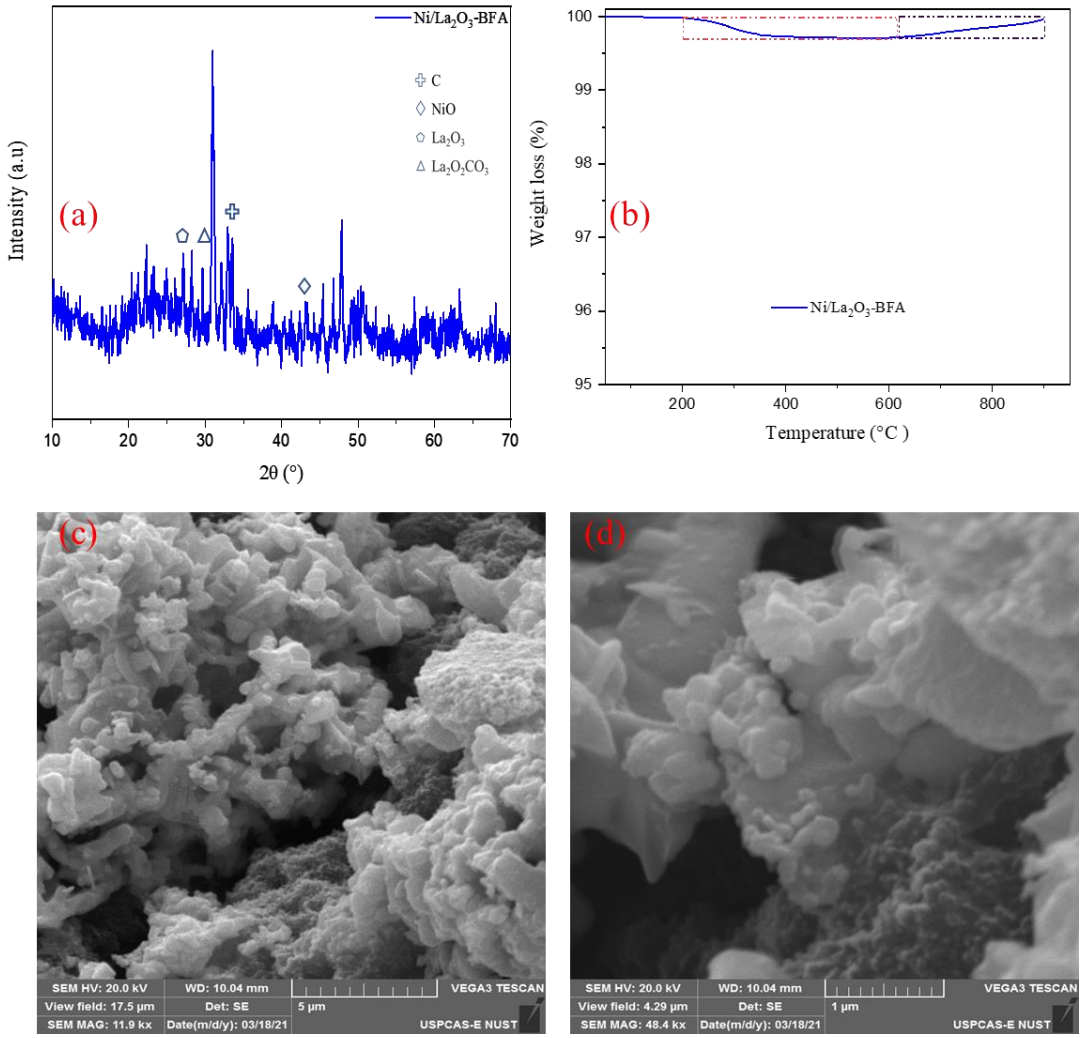

Figure 4-9 (a)Spent Ni/La_2O_3-BFA XRD (b) Spent Ni/La_2O_3-BFA TGA (c-d) SEM micrographs of spent Ni/ La_2O_3-BFA 5.0 µm and 1.0 µm after 30h TOS

4.3.2 TGA Analysis

The TGA profile of spent Ni/La_2O_3-BFA after 30 h on TOS is shown in Figure 4-9(b). The minute weight loss below 200 °C corresponds to the removal of volatile matter and moisture. The weight loss between 200-300 °C corresponds to a very small amount of carbidic carbon deposition that can be oxidized in the air [41]. The 0.24% weight gain observed after 650 °C is due to metallic active site oxidation [42] by different oxides present in BFA [11]. The weight gain may also correspond to the Si to SiC since Si was found in BFA [43].

4.3.3 SEM Analysis

In Figure 4-9(c-d) SEM micrographs of spent catalyst are shown which indicate a change in surface morphology from fresh to spent catalyst and shows La_2O_3 formed through carbonation from $La_2O_2CO_3$ to La_2O_3[44]. The change in morphology exhibit minute carbon deposition [45, 46]whose presence is also confirmed by XRD analysis.

4.3.4 EDX Analysis

EDX mapping of Spent catalyst is given in Figure 4-10 which confirm the formation of minute carbon while other peaks for Al, Si, Fe and Ca confirm the presence of already proved metallic oxides in BFA[11, 47].

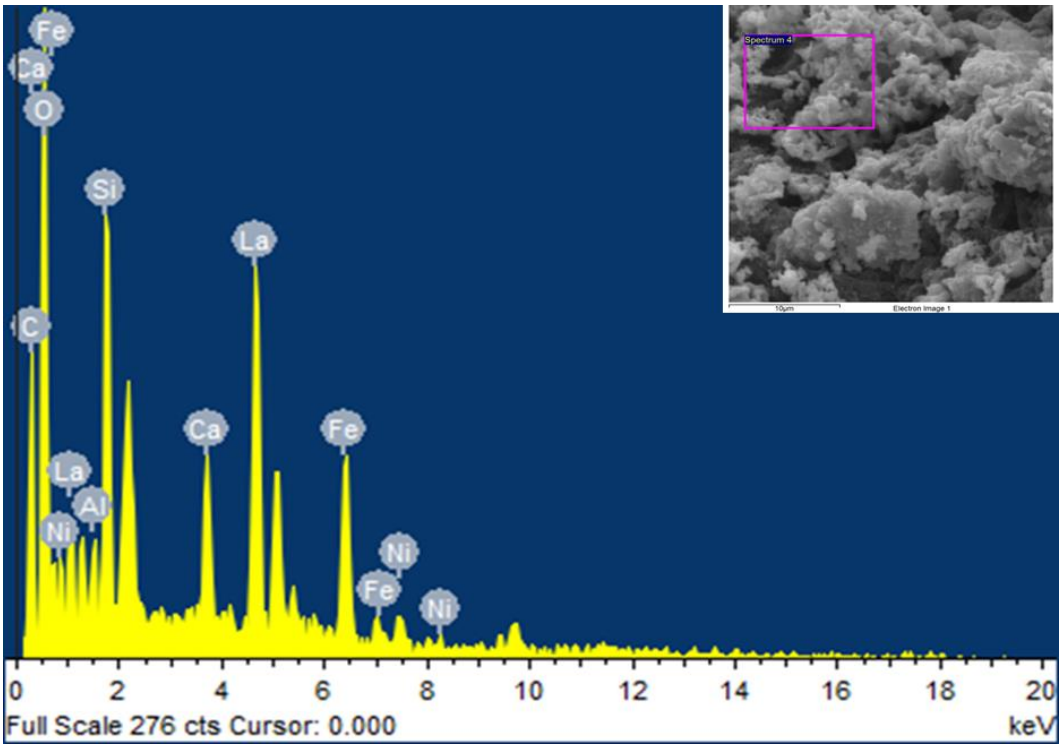

Figure 4-10 EDX elemental analysis of spent Ni/ La_2O_3-BFA

Summary

XRD, TGA, SEM, EDS, and FTIR were used to characterize the BFA sample, as well as the synthesized La_2O_3 and Ni-loaded catalyst. Various diffraction peaks for Fe_2O_3, Al_2O_3, MgO, and SiO2 can be observed in the BFA's XRD. The morphology of the BFA is exhibited by SEM, which indicates that it has a micro-flakes-like structure, making it good catalyst support for catalytic applications. SEM examination of the completed catalyst further demonstrates that the Ni and La2O3 are evenly distributed among the BFA micro-flakes. TGA demonstrated that the material was stable up to 900 °C, that makes it appropriate for applications that require high temperature. In FBR, the catalyst was tested for methane to syngas conversion by POM.

References

[1] A.I. Adeogun, A.E. Ofudje, M.A. Idowu, S.O. Kareem, Facile Development of Nano Size Calcium Hydroxyapatite Based Ceramic from Eggshells: Synthesis and Characterization, Waste and Biomass Valorization, 9 (2018) 1469-1473.

[2] Y. Yang, Z. Wei, Y.-l. Chen, Y. Li, X. Li, Utilizing phosphate mine tailings to produce ceramisite, Construction and Building Materials, 155 (2017) 1081-1090.

[3] N. Zhang, X. Chen, B. Chu, C. Cao, Y. Jin, Y. Cheng, Catalytic performance of Ni catalyst for steam methane reforming in a micro-channel reactor at high pressure, Chemical Engineering and Processing: Process Intensification, 118 (2017) 19-25.

[4] L. Wang, X. Cheng, Z. Wang, X. Zhang, C. Ma, NO reduction by CO over iron-based catalysts supported by activated semi-coke, The Canadian Journal of Chemical Engineering, 95 (2017) 449-458.

[5] C. Xu, Z. Yu, K. Yuan, X. Jin, S. Shi, X. Wang, L. Zhu, G. Zhang, D. Xu, H. Jiang, Improved preparation of electrospun MgO ceramic fibers with mesoporous structure and the adsorption properties for lead and cadmium, Ceramics International, 45 (2019) 3743-3753.

[6] T.P. Smirnova, L.V. Yakovkina, V.O. Borisov, M.S. Lebedev, Phase composition of nanosized oxide film structures based on lanthanum and scandium doped HfO_2, Journal of Structural Chemistry, 58 (2017) 1573-1580.

[7] C. Chen, J. Zhou, J. Geng, R. Bao, Z. Wang, J. Xia, H. Li, Perovskite $LaNiO_3/TiO_2$ step-scheme heterojunction with enhanced photocatalytic activity, Applied Surface Science, 503 (2020) 144287.

[8] A. Galal, N.F. Atta, M.A. Hefnawy, Lanthanum nickel oxide nano-perovskite decorated carbon nanotubes/poly(aniline) composite for effective electrochemical oxidation of urea, Journal of Electroanalytical Chemistry, 862 (2020) 114009.

[9] N.A.S. Nogueira, E.B. da Silva, P.M. Jardim, J.M. Sasaki, Synthesis and characterization of $NiAl_2O_4$ nanoparticles obtained through gelatin, Materials Letters, 61 (2007) 4743-4746.

[10] T. Li, S. Ni, X. Lv, X. Yang, S. Duan, Preparation of NiO–Ni/natural graphite composite anode for lithium ion batteries, Journal of Alloys and Compounds, 553 (2013) 167-171.

[11] M. Assad Munawar, A. Hussain Khoja, M. Hassan, R. Liaquat, S. Raza Naqvi, M. Taqi Mehran, A. Abdullah, F. Saleem, Biomass ash characterization, fusion analysis and its application in catalytic decomposition of methane, Fuel, 285 (2021) 119107.

[12] N. Sulaiman, Y. Yulizar, D. Bagus Apriandanu, Eco-friendly method for synthesis of La_2O_3 nanoparticles using Physalis angulata leaf extract, 2018.

[13] A. Pathan, K. Desai, Synthesis of La_2O_3 Nanoparticles using Glutaric acid and Propylene glycol for Future CMOS Applications, International Journal of Nanomaterials and Chemistry, 3 (2017) 21-25.

[14] W. Gu, J. Liu, M. Hu, F. Wang, Y. Song, $La_2O_2CO_3$ Encapsulated La_2O_3 Nanoparticles Supported on Carbon as Superior Electrocatalysts for Oxygen Reduction Reaction, ACS Applied Materials & Interfaces, 7 (2015) 26914-26922.

[15] J. Requies, M.A. Cabrero, V.L. Barrio, M.B. Güemez, J.F. Cambra, P.L. Arias, F.J. Pérez-Alonso, M. Ojeda, M.A. Peña, J.L.G. Fierro, Partial oxidation of methane to syngas over Ni/MgO and Ni/La_2O_3 catalysts, Applied Catalysis A: General, 289 (2005) 214-223.

[16] C. Guo, X. Zhang, J. Zhang, Y. Wang, Preparation of La_2NiO_4 catalyst and catalytic performance for partial oxidation of methane, Journal of Molecular Catalysis A: Chemical, 269 (2007) 254-259.

[17] S. Wang, G.Q. Lu, Reforming of methane with carbon dioxide over Ni/Al_2O_3 catalysts: Effect of nickel precursor, Applied Catalysis A: General, 169 (1998) 271-280.

[18] J. Kalembkiewicz, D. Galas, E. Sitarz-Palczak, The Physicochemical Properties and Composition of Biomass Ash and Evaluating Directions of its Applications, Polish Journal of Environmental Studies, 27 (2018).

[19] S. Karthikeyan, A.D. Raj, A.A. Irudayaraj, D.M.A. Raj, Effect of Temperature on the Properties of La_2O_3 Nanostructures, Materials Today: Proceedings, 2 (2015) 1021-1025.

[20] Z. Wei, H. Qiao, H. Yang, C. Zhang, X. Yan, Characterization of NiO nanoparticles by anodic arc plasma method, Journal of Alloys and Compounds, 479 (2009) 855-858.

[21] A.H. Khoja, M. Tahir, N.A. Saidina Amin, Evaluating the Performance of a Ni Catalyst Supported on La_2O_3-$MgAl_2O_4$ for Dry Reforming of Methane in a Packed Bed Dielectric Barrier Discharge Plasma Reactor, Energy & Fuels, 33 (2019) 11630-11647.

[22] A.S. Al-Fatesh, M.A. Naeem, A.H. Fakeeha, A.E. Abasaeed, Role of La_2O_3 as Promoter and Support in Ni/γ-Al_2O_3 Catalysts for Dry Reforming of Methane, Chinese Journal of Chemical Engineering, 22 (2014) 28-37.

[23] M. Fleys, Y. Simon, D. Swierczynski, A. Kiennemann, P.-M. Marquaire, Investigation of the Reaction of Partial Oxidation of Methane over Ni/La_2O_3 Catalyst, Energy & Fuels, 20 (2006) 2321-2329.

[24] R.K. Singha, A. Shukla, A. Yadav, L.N. Sivakumar Konathala, R. Bal, Effect of metal-support interaction on activity and stability of Ni-CeO_2 catalyst for partial oxidation of methane, Applied Catalysis B: Environmental, 202 (2017) 473-488.

[25] L. Mo, X. Zheng, Q. Jing, H. Lou, J. Fei, Combined Carbon Dioxide Reforming and Partial Oxidation of Methane to Syngas over Ni−La_2O_3/SiO_2 Catalysts in a Fluidized-Bed Reactor, Energy & Fuels, 19 (2005) 49-53.

[26] Y.-g. Chen, J. Ren, Conversion of methane and carbon dioxide into synthesis gas over alumina-supported nickel catalysts. Effect of Ni-Al_2O_3 interactions, Catalysis Letters, 29 (1994) 39-48.

[27] B.S. Liu, C.T. Au, Carbon deposition and catalyst stability over La_2NiO_4/γ-Al_2O_3 during CO_2 reforming of methane to syngas, Applied Catalysis A: General, 244 (2003) 181-195.

[28] A.G. Dedov, A.S. Loktev, D.A. Komissarenko, G.N. Mazo, O.A. Shlyakhtin, K.V. Parkhomenko, A.A. Kiennemann, A.C. Roger, A.V. Ishmurzin, I.I. Moiseev, Partial oxidation of methane to produce syngas over a neodymium–calcium cobaltate-based catalyst, Applied Catalysis A: General, 489 (2015) 140-146.

[29] Q. Duan, J. Wang, C. Ding, H. Ding, S. Guo, Y. Jia, P. Liu, K. Zhang, Partial oxidation of methane over Ni based catalyst derived from order mesoporous $LaNiO_3$ perovskite prepared by modified nanocasting method, Fuel, 193 (2017) 112-118.

[30] Y. Ma, Y. Ma, Z. Zhao, X. Hu, Z. Ye, J. Yao, C.E. Buckley, D. Dong, Comparison of fibrous catalysts and monolithic catalysts for catalytic methane partial oxidation, Renewable Energy, 138 (2019) 1010-1017.

[31] M. Goenka, C. Nihal, R. Ramanathan, P. Gupta, A. Parashar, J. Joel, Automobile Parts Casting-Methods and Materials Used: A Review, Materials Today: Proceedings, 22 (2020) 2525-2531.

[32] Z. Zhang, X.E. Verykios, Carbon dioxide reforming of methane to synthesis gas over Ni/La_2O_3 catalysts, Applied Catalysis A: General, 138 (1996) 109-133.

[33] J.C.S. Araújo, L.F. Oton, A.C. Oliveira, R. Lang, L. Otubo, J.M.C. Bueno, On the role of size controlled Pt particles in nanostructured Pt-containing Al_2O_3 catalysts for partial oxidation of methane, International Journal of Hydrogen Energy, 44 (2019) 27329-27342.

[34] M. Gil-Calvo, C. Jimenez-Gonzalez, B. de Rivas, J.I. Gutierrez-Ortiz, R. Lopez-Fonseca, Effect of Ni/Al molar ratio on the performance of substoichiometric $NiAl_2O_4$ spinel-based catalysts for partial oxidation of methane, Appl Catal B-Environ, 209 (2017) 128-138.

[35] A. Hamza Fakeeha, Y. Arafat, A. Aidid Ibrahim, H. Shaikh, H. Atia, A. Elhag Abasaeed, U. Armbruster, A. Sadeq Al-Fatesh, Highly Selective Syngas/H_2 Production via Partial Oxidation of CH_4 Using (Ni, Co and Ni–Co)/ZrO_2–Al_2O_3 Catalysts: Influence of Calcination Temperature, Processes, 7 (2019) 141.

[36] J. Requies, M.A. Cabrero, V.L. Barrio, M.B. Guemez, J.F. Cambra, P.L. Arias, F.J. Perez-Alonso, M. Ojeda, M.A. Pena, J.L.G. Fierro, Partial oxidation of methane to syngas over Ni/MgO and Ni/La_2O_3 catalysts, Appl Catal a-Gen, 289 (2005) 214-223.

[37] A.A. Ibrahim, W.U. Khan, F. Al-Mubaddel, A.S. Al-Fatesh, S.O. Kasim, S.L. Mahmud, A.A. Al-Zahrani, M.R.H. Siddiqui, A.H. Fakeeha, Study of Partial Oxidation of Methane by Ni/Al_2O_3 Catalyst: Effect of Support Oxides of Mg, Mo, Ti and Y as Promoters, Molecules, 25 (2020) 5029.

[38] B. Priyono, A.R. Bachtiar, H. Abraham, M.R. Nugraha, Faizah, A.Z. Syahrial, J.F. Fatriansyah, A. Subhan, Optimizing Performance of ZnO Nanorod and Activated Carbon as a Composite Anode for Lithium-Ion Batteries, Materials Science Forum, 1000 (2020) 31-40.

[39] M.K. Baig, H. Soleimani, N. Yahya, M. Sabet, Magnetic Behavior of Ni/NiO Core–Shell Nanoparticles under Electromagnetic Waves for Oil–Water Interfacial Tension Reduction, Journal of Materials Engineering and Performance, 28 (2019) 5882-5889.

[40] L. Wang, Y. Ma, Y. Wang, S. Liu, Y. Deng, Efficient synthesis of glycerol carbonate from glycerol and urea with lanthanum oxide as a solid base catalyst, Catalysis Communications, 12 (2011) 1458-1462.

[41] C. Guo, J. Zhang, X. Zhang, Comparative study of $LaNiO_3$ and La_2NiO_4 catalysts for partial oxidation of methane, Reaction Kinetics and Catalysis Letters, 95 (2008) 89-97.

[42] G.S. Gallego, J.G. Marín, C. Batiot-Dupeyrat, J. Barrault, F. Mondragón, Influence of Pr and Ce in dry methane reforming catalysts produced from $La_{1-x}A_xNiO_{3-\delta}$ perovskites, Applied Catalysis A: General, 369 (2009) 97-103.

[43] G.G. Meric, H. Arbag, L. Degirmenci, Coke minimization via SIC formation in dry reforming of methane conducted in the presence of Ni-based core-shell microsphere catalysts, International Journal of Hydrogen Energy, 42 (2017) 16579-16588.

[44] K. Mustofa, Y. Yulizar, A. Saefumillah, D.O.B. Apriandanu, La2O3 nanoparticles formation using Nothopanax scutellarium leaf extract in two-phase system and photocatalytic activity under UV light irradiation, IOP Conference Series: Materials Science and Engineering, 902 (2020) 012018.

[45] S. Moogi, I.-G. Lee, J.-Y. Park, Effect of La_2O_3 and CeO_2 loadings on formation of nickel-phyllosilicate precursor during preparation of Ni/SBA-15 for hydrogen-rich gas production from ethanol steam reforming, International Journal of Hydrogen Energy, 44 (2019) 29537-29546.

[46] N. Habibi, M. Rezaei, N. Majidian, M. Andache, CH_4 reforming with CO_2 for syngas production over La_2O_3 promoted Ni catalysts supported on mesoporous nanostructured γ-Al_2O_3, Journal of Energy Chemistry, 23 (2014) 435-442.

[47] B. Nabgan, M. Tahir, T.A.T. Abdullah, W. Nabgan, Y. Gambo, R. Mat, I. Saeh, Ni/Pd-promoted Al_2O_3–La_2O_3 catalyst for hydrogen production from polyethylene terephthalate waste via steam reforming, International Journal of Hydrogen Energy, 42 (2017) 10708-10721.

Chapter 5
Conclusions and Recommendations

5.1 Conclusions

- BFA effective utilisation produced by biomass power plants was a major challenge. The biomass derived Ni/La_2O_3-BFA is synthesized and employed effectively for POM to Syngas in a fixed bed reactor.
- The physicochemical properties of BFA have been examined to resolve this issue, and it has been determined that BFA is best suited as catalyst support in various technologies. The existence of several metal oxides in BFA make it a viable catalyst support material
- The addition of Ni and La_2O_3 enhanced the methane conversion from 55% to 85% and H_2/CO from 1.4 to 2.0 molar ratio.
- The biomass-derived catalyst is economical and greener approach for POM

5.2 Recommendations

POM is the most effective method and a greener route for syngas production. POM could become more efficient using stable and economical catalyst. However, the major challenge associated with the given process is the hot spot formation that results in the sintering of catalyst. Furthermore, BFA has better physicochemical properties that could overcome the shortcomings due to hotspot formation and coke deposition. It should be used for catalytic purposes with different promoters in the future. For maximum conversion of methane and hydrogen yield, the reactor design should be considered along with the experimental parameter. The kinetic study and reaction mechanism for biomass derived catalyst should be investigated.

APPENDIX-PUBLICATIONS

frontiers

Synthesis of biomass fly ash (BFA) co-supported Ni/La2O3 cat-alyst for partial oxidation of methane to hydrogen rich syngas production

Amin Ul Hasanat[1], Asif Hussain Khoja[1,*], Majid Ali[1], Salman Raza Naqvi[2], Rahat Javaid[3], Umair Yaqub Qazi[4], Sami M. Ibn Shamsah[5]

[1] Fossil Fuels Laboratory, Department of Thermal Energy Engineering, U.S.-Pakistan Centre for Advanced Studies in Energy (USPCAS-E), National University of Sciences & Technology (NUST), Sector H-12 Islamabad (44000), Pakistan.
[2] School of Chemical and Materials Engineering, National University of Sciences & Technology (NUST), Sector H-12 Islamabad (44000), Pakistan.
[3] Renewable Energy Research Center, Fukushima Renewable Energy Institute, National Institute of Advanced Industrial Science and Technology, AIST, 2-2-9 Machiikedai, Koriyama, Fukushima 963-0298, Japan.
[4] Department of Chemistry, College of Science, University of Hafr Al Batin. P.O Box 1803 Hafr Al Batin 39524, Kingdom of Saudi Arabia.
[5] Department of Mechanical Engineering, College of Engineering, University of Hafr Al Batin.
P.O Box 1803, Hafr Al Batin 31991, Kingdom of Saudi Arabia

* Correspondence: asif@uspcase.nust.edu.pk

Keywords: ***Partial oxidation of methane (POM); Syngas; Biomass fly ash; La_2O_3; Hydrogen production .***

Abstract

In this study, the biomass fly ash (BFA) supported Ni/La_2O_3 catalyst is synthesized to produce syngas via partial oxidation of methane (POM). BFA support was modified using laboratory synthesized La_2O_3 and loaded nickel (Ni) as active metal through the wetness impregnation technique. The Ni/La_2O_3-BFA catalyst was characterized by X-ray diffraction (XRD), scanning electron microscopy (SEM), energy-dispersive X-ray spectroscopy (EDX), thermogravimetric analysis (TGA) and Fourier transform infrared spectroscopy (FTIR) to investigate its suitability for POM reaction. The crystalline structure and enhanced thermal stability of Ni/La_2O_3-BFA make it suitable for POM reaction. The presence of various metal oxides such as Al_2O_3, Fe_2O_3, MgO, and SiO_2 in BFA makes it a more suitable support material for POM. The synthesized Ni/La_2O_3-BFA catalyst remained stable for 30 h time on stream (TOS) during POM at 850 °C. The experimental study demonstrated that the addition of La_2O_3 promoter and active metal Ni to the BFA improved the CH_4 conversion from 55% to 85% and consequently improved H_2/CO ratio from 1.4 to 2.0. The catalytic performance of BFA supported catalyst shows its potential to be adopted for catalytic application, that is a greener and waste-based alternative catalyst for methane reduction.